General Disclaimer

One or more of the Following Statements may affect this Document

- This document has been reproduced from the best copy furnished by the organizational source. It is being released in the interest of making available as much information as possible.

- This document may contain data, which exceeds the sheet parameters. It was furnished in this condition by the organizational source and is the best copy available.

- This document may contain tone-on-tone or color graphs, charts and/or pictures, which have been reproduced in black and white.

- This document is paginated as submitted by the original source.

- Portions of this document are not fully legible due to the historical nature of some of the material. However, it is the best reproduction available from the original submission.

Produced by the NASA Center for Aerospace Information (CASI)

EXPERIMENTAL   INVESTIGATION   AND
MODEL   DEVELOPMENT   OF   THE   SKYLAB
ATM   SECONDARD   NICKEL-CADMIUM
BATTERIES

by

W. W. Kirsch

40M 22412

ABSTRACT

This report presents the second half of a Ni-Cd battery evaluation program which investigated the performance of cells and batteries to be used on the Skylab Apollo Telescope Mount (ATM). The first half of the program determined the cyclic battery controls to be used on the ATM batteries. All the work described was done for NASA-MSFC.

The goal of the battery evaluation program was to develop cell and battery performance models which could be used to predict the performance of the secondary Ni-Cd batteries on the ATM. Two areas of battery operation were considered for the models. These were capacity degradation, and charge acceptance characteristics. Mathematical models for each of these operating areas were developed. The models were based on data acquired from two separate test programs, each designed to provide a range of data for one of the models. The test variable performance ranges were $0^{\circ}C$ to 30° Celsius, 10 percent to 40 percent depth-of-discharge (DOD), and 0.1C to 1.0C amperes charge rate where C is the rated battery capacity.

The capacity degradation model describes the expected usable battery capacity as a function of time, temperature, and depth-of-discharge. It reflects the steady-state, and transient temperature and DOD conditions. Time is presented in terms of cyclic operation with each cycle being composed of a 58 minute available charge time followed by a 36 minute discharge.

iv

40M 22412

The charge acceptance model describes the cell charge acceptance as a function of charge rate, temperature, and state of charge. It is primarily useful when a complete recharge cannot be achieved during one orbit.

The models were designed for computer use although simplified manual calculations are easily performed. The models can be used to predict expected performance or to compare real time performance during flight. The models have also been designed to facilitate modification if battery changes occur as a result of cell design improvements or a change in vendor.

40M 2.2.4/2

40M 22412

LIST OF ILLUSTRATIONS

40M 22412

LIST OF TABLES

40M 22412

CHAPTER I

INTRODUCTION

The high degree of success demonstrated by the NASA space program is in part due to the effective use of reliable electrical energy storage devices, namely batteries, both primary and secondary. Batteries were selected during the initial phases of the space program because of their high degree of development and their demonstrated reliability. For short missions lasting several days, primary batteries were used[1]. Orbital missions, such as satellites, used secondary batteries as a primary power source in conjunction with a solar energy conversion device.

Since most orbiting satellites are designed for long life missions, the battery most often chosen as the primary electrical energy storage source is a secondary Nickel-Cadmium (Ni-Cd) battery. This battery was chosen because of its demonstrated long cycle life, and its low failure rate[2]. For the unmanned satellites, the load profiles have been fairly constant resulting in a constant battery discharge during orbital eclipse periods and well defined battery charge times and conditions during sunlight periods. This type of constant cyclic regime has been found to be ideal for Ni-Cd battery operation[3]. It allows the battery to be trickle charged for long periods in a manner that does not cause thermal or electrical strain to the batteries. However well the batteries functioned in the unmanned orbiting satellites, they did not require the reliability and performance standards required of manned satellites.

1

40M22412

With the advent of the manned mission, in particular the NASA
Skylab ATM program, new demands have been placed upon the Ni-Cd
battery. Primary power in the Skylab utilizes space qualified
state-of-the-art solar arrays and Ni-Cd batteries. The manned
status and the orbital conditions of the Skylab mission impose new
demands on the performance characteristics of the primary power
components, primarily the batteries. The mission profile specified
cyclic load variations which would range from a 10 percent battery
depth-of-discharge during mission storage modes up to a 60 percent
battery depth-of-discharge during earth resources experiments and
rendezvous maneuvers[4]. Battery thermal output restrictions, in
addition to limited charging time, further complicated the
operating restraints of the Ni-Cd batteries. Safety requirements
have also increased as a result of the manned status of the mission.

Because of the increased operating demands placed on the battery,
new and improved electrical and thermal controls had to be devised.
For the ATM portion of Skylab, thermal considerations were the most
important since the ATM batteries were passively cooled. The
thermal limits required that the batteries be operated at maximum
achievable efficiency. Since discharge efficiencies have been
demonstrated to be constant, the cyclic efficiencies must be
maximized via optimized charging techniques[6]. All battery performance
optimizing, however, must be within the safe and reliable operating
range of the batteries. After the controls have been optimized,
the battery performance should be characterized throughout its

expected operating range. This second task is important for proper mission planning because battery performance degrades during the mission and information regarding instantaneous battery conditions is often desirable.

Control of the ATM Skylab batteries within the Skylab mission constraints was investigated from 1958 through 1970 and was reported in Reference 7. A summary of the results of that investigation is

1. Usable battery capacity degrades as a function of cyclic time, temperature, and depth-of-discharge.

2. Battery charge acceptance is more efficient at high charge rates than low charge rates. Charge acceptance is also temperature dependent.

3. Maximum battery voltage limits during charge are temperature dependent. This limit is imposed to preclude the evolution of internal cell hydrogen pressure which cannot be readily recombined. The actual battery voltage limits were empirically determined.

In addition to the operational battery limits, the Skylab mission also imposed operating restraints. The primary restraints were:

1. Battery charging time was limited to approximately 58 minutes.

2. Available battery charging power was limited by solar array size and by the system load. During earth resources experiments, when high solar array temperatures

40M 22412

or high load demands occur, the battery would be charged at very low rates and would very likely not be fully charged in the cycle[8].

These restraints, both control and mission, and a desire for optimum performance, resulted in a need to predict expected performance as well as to check real time performance. Since usable battery capacity degrades, capacity is essentially a consumable item and expected capacity degradation characterisitics are needed for mission planning. Likewise during cycles where the recharge is incomplete, an accounting of the battery state of charge is necessary for proper planning.

At the outset, the information need was to define the battery performance variables in terms of measureable performance parameters. The variables are:

1) Battery Capacity Availability which is defined as:

Percent Rated Capacity (PRC)

$$PRC = \frac{Available\ Capacity\ (A\text{-}hr)}{Rated\ Battery\ Capacity\ (A\text{-}hr)} \times 100$$

2) Battery Charge Acceptance which is defined as:

$$Charge\ Acceptance = \frac{Ampere\ hours\ out}{Ampere\ hours\ in}$$

The measurable performance parameters are:

40M 2-24-12

1)   Battery Cyclic History where each cycle equals 36 minutes of discharge followed by 58 minutes of available charge time.

2)   Battery Current in amperes.

3)   Battery Temperature in degrees Celsius.

A literature search did not reveal any current programs or results which would provide inputs to battery performance models. A two part program was therefore initiated. The first part consisted of the design, performance, and evaluation of experiments which measured battery performance within the expected mission operating conditions. The second part of the program used the data as a set of boundary conditions for the development of mathematical battery performance models. These two parts are discussed in chapters two and three respectively.

40M 22-412

EXPERIMENTAL PROGRAM

Two independent battery tests were conducted to generate essential modeling data: Capacity Degradation and Charge Acceptance. This approach was taken to optimize the use of available time, test facilities, and test specimens.

The "Capacity Degradation" test established usable battery capacity, as a function of battery load, temperature, and cyclic history. An additional function was to determine the battery capacity response to load and temperature changes. Resulting data, when modeled, enabled accurate prediction of the available battery capacity at any time during the ATM mission when the battery has completed a charge. Stated another way, this test reflected the expected battery capacity degradation response characteristics.

Battery "Charge Acceptance" test data is primarily required during the ATM mission earth resources experiments when the battery cannot always be fully recharged during one orbit. The lack of recharge is caused by limited solar array power and high battery discharge depths. Under these conditions it becomes important to predict instantaneous state of charge and the effects of charging or discharging. The charge acceptance data determined charge acceptance as a function of temperature, state of charge, and charge rate.

Test Cycle

All cyclic operation was conducted by subjecting the test specimen to a typical simulated ATM cycle as shown in Figure 1.

40M 2 2 4/2
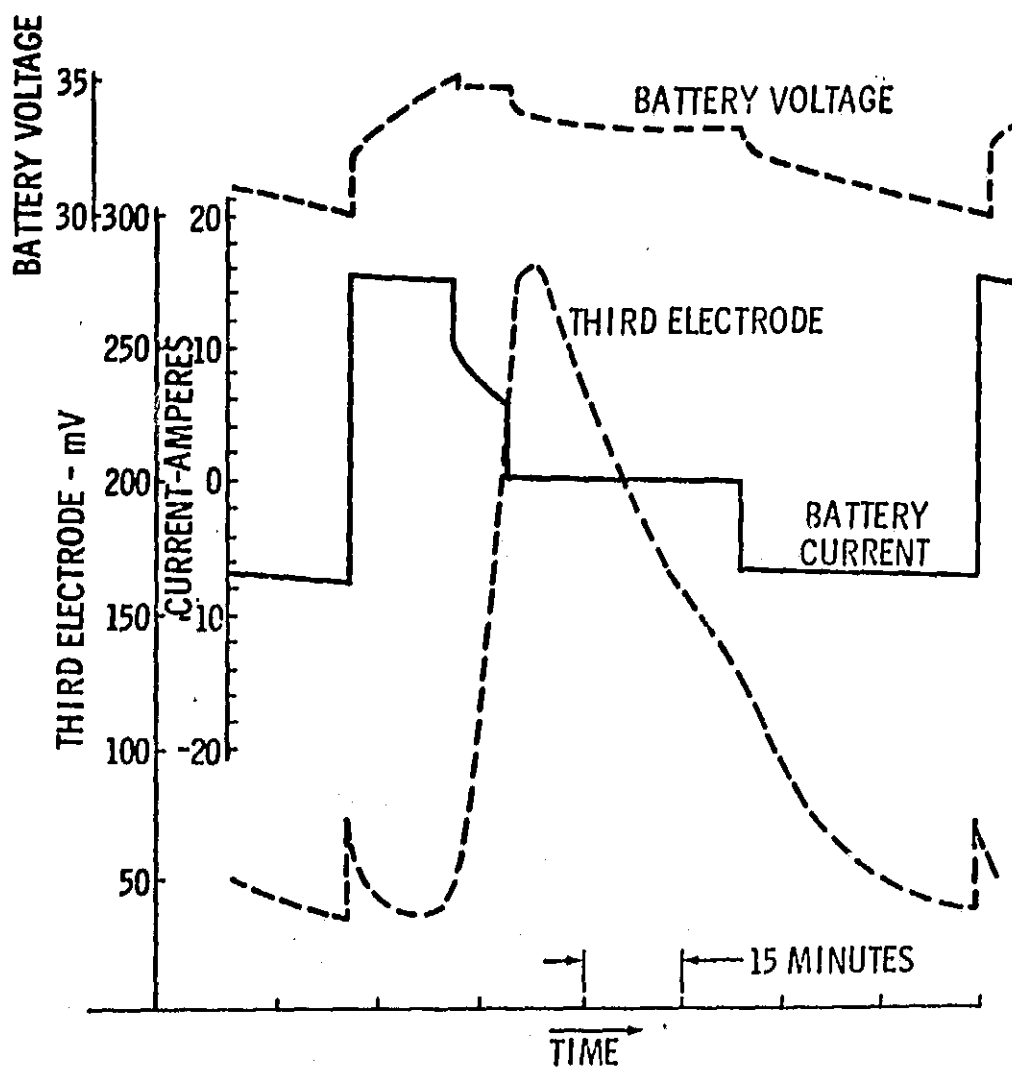
Figure 1. Simulated Orbital Cycle

40M22412

The 94-minute ATM orbital cycle is subdivided into a 58-minute charge and a 36-minute discharge. A charge consists of a 15-ampere constant current charge until the battery voltage reaches a temperature compensated maximum level. The charge is then converted from a constant current mode to a constant voltage mode which is 0.85 volts less than the maximum battery voltage. Charge termination occurs when the third electrode signal, generated by the cell nearest the negative battery terminal, reaches 200 millivolts. The third electrode signal is proportional to internal cell oxygen pressure which in turn is proportional to the cell state of charge. The empirically determined[7] maximum allowable ATM battery voltage as a function of temperature is shown in Figure 2.

Test Specimens

All parametric tests were conducted with the two types of AB12 cells shown in Table I. Capacity degradation tests were performed with non-flight AB12 cells. Cyclic data and charge efficiency data was acquired with AB12-G flight cells. No measurable capacity differences were noted between the two types of cells thereby insuring the validity of the capacity degradation tests.

Capacity Degradation

The capacity degradation test was designed to measure the capacity degradation as a function of cumulative cyclic operation, cyclic depth-of-discharge (DOD) and battery temperature. The DOD is defined as the ampere hours removed during discharge divided by the rated battery capacity (20 A-hr). The test configuration as

4OM 22412
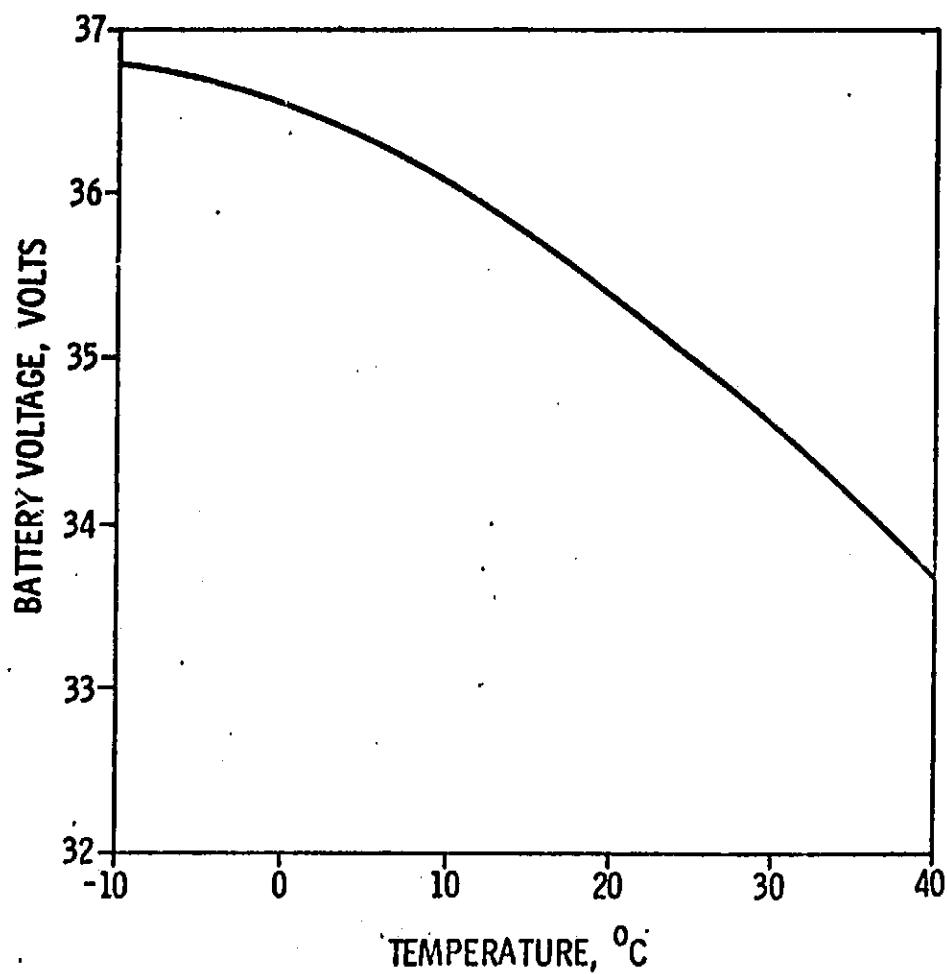
Figure 2. Battery Voltage Temperature Compensation

40M 2.24 / 2

TABLE I

CELL DESCRIPTION

Leading Particulars	Type AB12	Flight Type AB12G
Capacity (Ampere-hour)		
Rated	20	20
Average	25	25
Third Electrode	Type C*	Type C*
Recombination Electrode	Yes	Yes, 175 ohms
Precharged Cd Plate/Plate Ratio	Yes/1.2	Yes/1.45
Electrolyte Volume (34% KOH)	67 cc	70 cc
Weight (grams)	899	1043.28 max
Dimensions (centimeters)		
Height	18.176 ± 0.04	18.12
Width	7.61	7.62 ± 0.38
Thickness	2.29	2.29

*The third electrode in the flight type AB12 is located between the top and approximately one third down the 2.29 centimeter cell face. On the older cell, the third electrode was located on the 7.62 centimeter cell face.

40M 22412

noted in Table II is a Latin Square design. The Latin Square

design was chosen because it maximizes the information within a

minimum time frame and with a minimum number of test specimens.

The test specimens consisting of four, 4-cell AB12 batteries

were used during each 8 week period noted in Table II. Four

thermal chambers, each containing a battery, were operated

simultaneously. At any given time, all test batteries were sub-

jected to an equal depth-of-discharge but were maintained at

different temperatures. The order in which the four 8-week test

phases were conducted is noted in the table.

Test batteries were initially adjusted for proper cyclic

operation at Cycle 1. A typical cycle is shown in Figure 1.

During subsequent cycles, each battery was allowed to respond to its

respective test conditions. Planned test parameter changes

occurred approximately every 800 cycles. Test equipment failures

and other interruptions, however, resulted in modifications to

this procedure. These modifications did not appear to affect the

test results. Battery capacity data was acquired by discharging

at a 10-ampere rate until the voltage of any cell decreased to 1.0

volt. Normal cyclic operation was resumed following an ATM type

charge which was maintained until the third electrode signal

terminated the charge.

Capacity degradation test results are shown in Figure 3 and 4.

Measured capacity at any time has been normalized to the 20 ampere-

40M22412

TABLE II

CAPACITY DEGRADATION TEST CONFIGURATION

TESTING TIME	PERCENT DOD	TEMPERATURE			
		0°C	10°C	20°C	30°C
8 WK_1	20%	B_3	B_2	B_1	B_4
8 WK_2	25%	B_4	B_1	B_2	B_3
8 WK_3	10%	B_2	B_4	B_3	B_1
8 WK_4	40%	B_1	B_3	B_4	B_2

40M22412
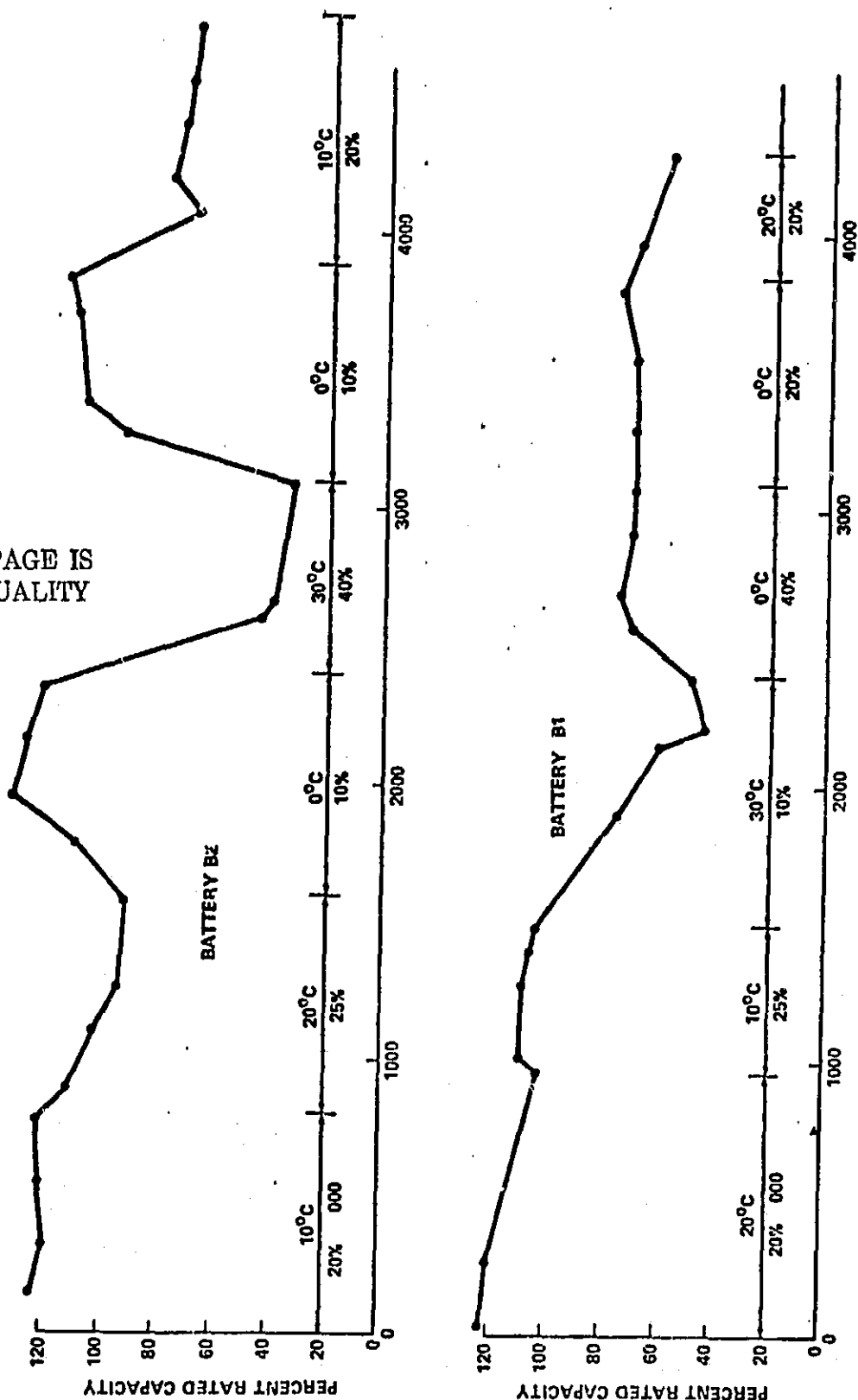
Figure 3. Measured Battery Capacity
(20 A-Hr GE-AB12 Cell)
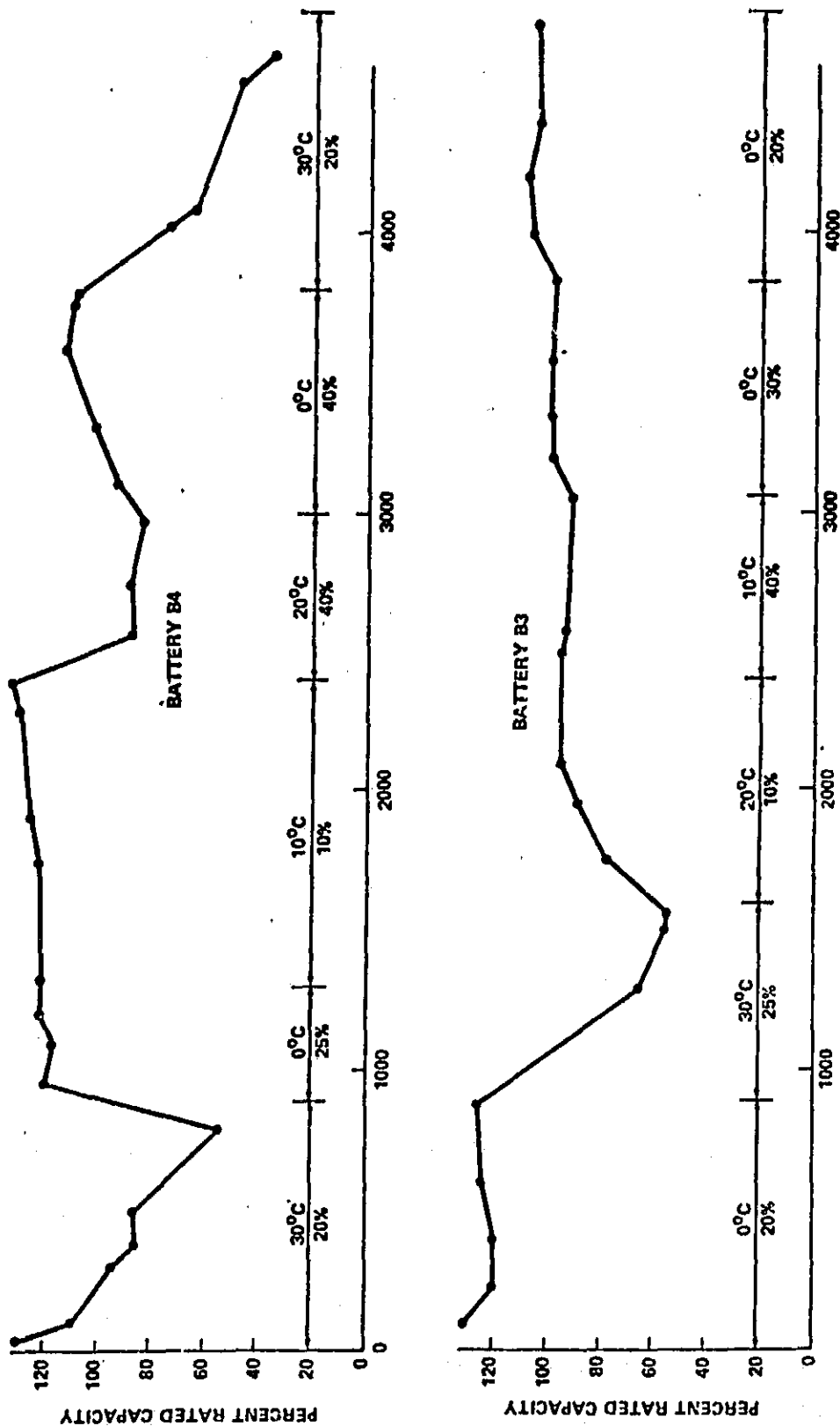
40M 22412

Figure 4. Measured Battery Capacity
(20 A-Hr GE-AB12 Cell)

40M 22412

hour rated battery capacity in units of percent rated capacity (PRC = $\frac{\text{Measured capacity}}{20}$ X 100). The depth-of-discharge is normalized in a like manner. The results of the capacity test indicate several significant factors:

1. A high level of usable capacity is maintained when the temperature is kept below 10 degrees C. After 4000 simulated ATM cycles, which is equivalent to an 8-month ATM mission, more than 70 percent of the battery capacity remains available when the temperature is at 10 degrees C or less.

2. A high rate of capacity degradation occurs when the battery temperature is above 20 degrees C.

3. A recovery of usable capacity occurs when the temperature is decreased. This is the only recovery technique observed that is useful and practical in present Ni-Cd battery space applications.

4. A depth-of-discharge effect on the steady state degradation is minor.

Expected capacity degradation characteristics between 0 degrees C and 30 degrees C are shown in Figure 5. These curves were developed from the test data in Figures 3 and 4. The development is noted in the next chapter. It is important to note that the degradation rates do not necessarily reflect cell failure rates. Cell failure modes were not investigated in this test program.
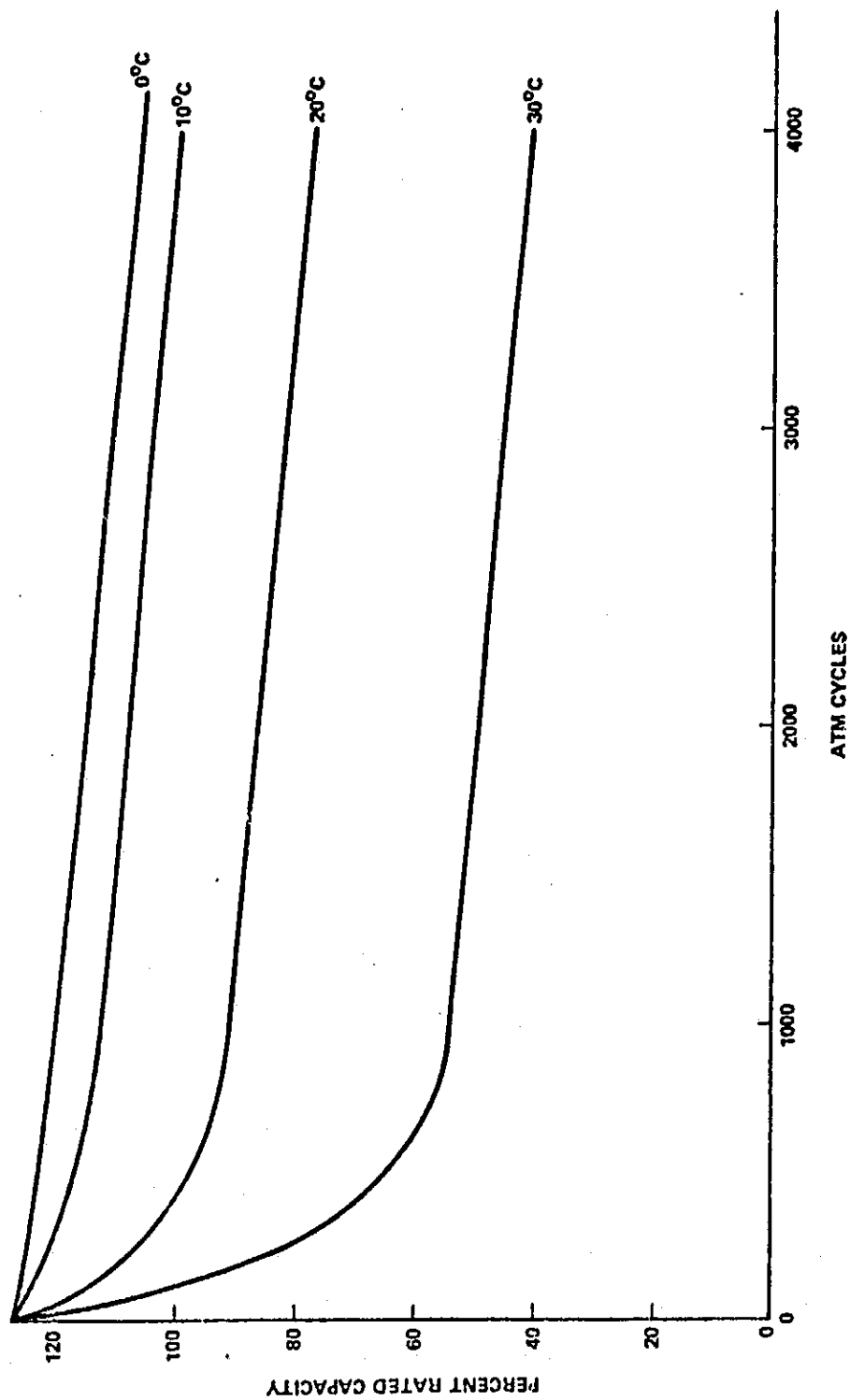
40M 22412

Figure 5. Expected Capacity Degradation
Temperature and DOD Constant
(20% DOD)

40M22412

Charge Acceptance

The charge acceptance test was conducted by charging a depleted battery at a given rate to a given state of charge and then discharging the battery at a 1.0 ampere rate. The charge acceptance efficiency is then defined as the ratio of ampere hours out to ampere hours in times 100. It is important to note that as a result of this test procedure each data point is the average, not the instantaneous, charge efficiency at that state of charge. The test configuration and the resulting data are shown in Table III. The data is shown in graphical form in Figures 6 and 7.

There are several reasons for the somewhat unorthodox test configuration. The primary reason is as a result of Bauer's[2] compilation of state-of-the-art Ni-Cd battery data. Based on highly smoothed data he indicated the charge efficiency was proportional to charge rate but inversely proportional to battery temperature and battery state of charge. This prompted more test data to be acquired at high temperatures, high states of charge and low charge rates. Another reason for the unorthodox test configuration is the test result use factor and the impact of the available test time and test facilities. The low use factor occurred because tests at high states of charge were up to 30 hours in duration. Any power failure or equipment failure, especially during unattended night time operation, negated the test. These factors

40M 22412

TABLE III

CHARGE ACCEPTANCE TEST DATA 18

Charge Rate (Amperes)	STATE OF CHARGE (% Rated Capacity) (15°C)				
	5	100	130	140	150
0.5					
1.0	94				
2.0	97				
5.0	99				

Charge Rate (Amperes)	STATE OF CHARGE (% Rated Capacity) (25°C)				
	5	100	130	140	150
0.5			67		
1.0	90.5	87.5	80.6		
2.0	94.3	93.3	88		
5.0	99.	95.5	89		80

Charge Rate (Amperes)	STATE OF CHARGE (% Rated Capacity) (35°C)				
	5	100	130	140	150
0.5			87.3		
1.0	93			49.5	
2.0	92				
5.0	97	94	89.3	81.3	
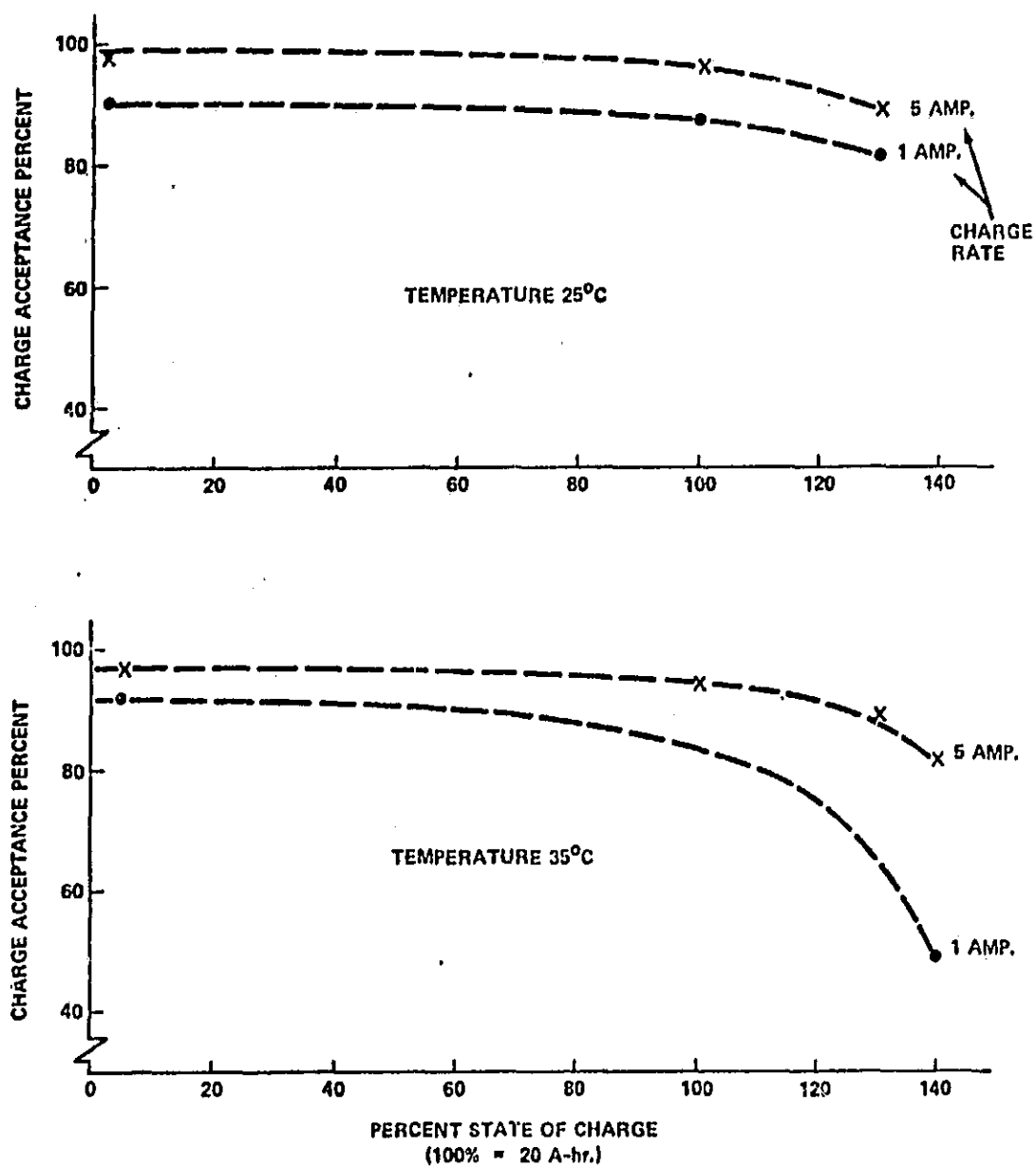
40M 22412

Figure 6.   Average Charge Acceptance
Characteristics
20 A-hr GE AB12-G Battery
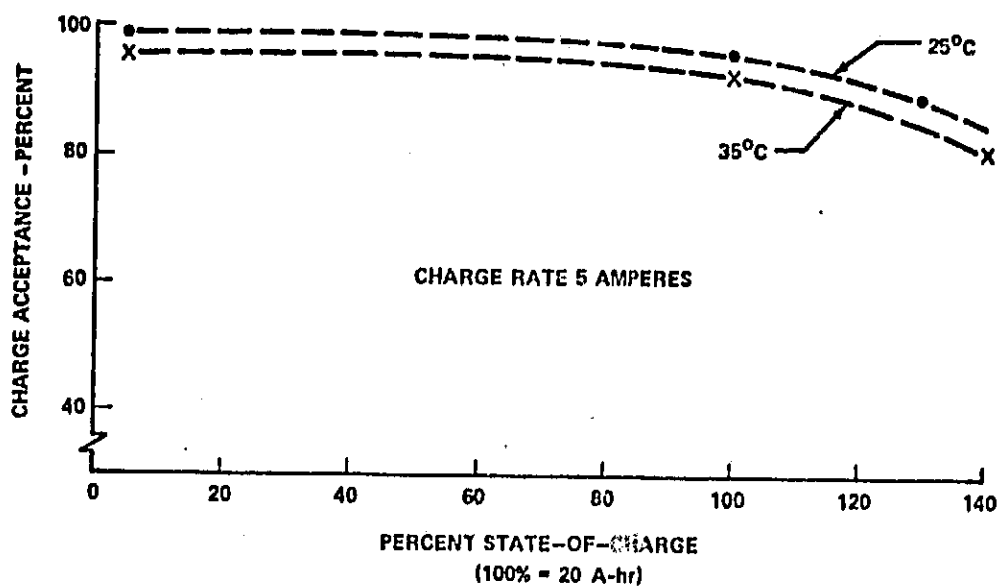
Figure 7.   Average Charge Acceptance Characteristics
20 A-hr GE AB12-G Battery

coupled with test scheduling based on a 5 day, no overtime, work week strained the total testing time.

Experimental Program Summary

The significant factors of the capacity degradation test indicate that a high level of usable capacity is maintained when the battery temperature is kept below 10 degrees C. Also, whenever usable capacity has degraded as a result of high temperature operation, a capacity recovery can be achieved by cyclic operation at 10 degrees C or less.

Results of the charge acceptance test concur with Bauer's finding. High levels of charge acceptance occur at low states of charge, low temperatures, and high charge rates. Conversely, the charge acceptance decreases as the state of charge increases, the charge rate decreases, and the temperature increases.

This initial battery performance investigation was conducted in two independent phases to minimize the testing time, maximize use of the test facility, and to provide an information and data base from which a subsequent program could be planned. The subsequent program will investigate: degradation of cell voltages as a function of temperature, depth-of-discharge, and cumulative cyclic history; the impact of storage modes; and the effect of various forms of intermittent battery operation.

A special area of battery performance requires mentioning, namely cell life characteristics. It appears from a review of

40M 22412

battery literature that cell life is independent of capacity
degradation but is dependent on the cyclic depth-of-discharge and
the recharge methods.   No substantiating data, however, has been
acquired during this test program.   A performance model describing
the expected cell and battery life characteristics would be highly
desirable and will be investigated in the subsequent programs.

40H 22.412

MODEL FORMULATION

Capacity Degradation

From a functional viewpoint, the most important battery para-
meter is the usable capacity available at any time. The capacity
degradation characteristics of the ATM Ni-Cd batteries are of great
concern because excessive loss of usable capacity, especially if
unknown, could seriously affect the mission. A model which
quantifies the degradation characteristics has been developed. The
model is based on the experimental data previously discussed and
shown in Figures 3 and 4. It is, therefore, primarily a model of
the ATM 20 ampere-hour Ni-Cd battery, but the methods used to
develop the model are general.

The percent rated capacity (PRC) of the ATM batteries, Figures
3 and 4, indicates that the capacity is a function of cycles,
temperature, and depth-of-discharge.

PRC = f (cycles, T, DOD)

Since there was no capacity degradation model discovered in
the literature on which to base this effort, the approach used to
form this model was to assume a form and then to apply appropriate
tests to see if the data did indeed fit the assumed model.

Before assuming a form, the development was subdivided into
two phases: steady state capacity, and transient capacity. Steady
state capacity (PRC_{ss}) is defined as the measured capacity after
more than 500 continuous cycles at constant temperature and DOD
have been accumulated. The steady state model development was

40M22412

initiated by tabulating the steady state data from Figures 3
and 4 into Table IV. A plot of this data is shown in Figure 8.

The PRC_{ss} in the figure shows a capacity decrease as a
function of cumulative cycles, battery temperature, and cyclic
depth-of-discharge (DOD). Assuming these three parameters are
independent, they can be described by:

$$PRC_{ss} = f \text{ (cycles)} + f \text{ (temperature)} + f(DOD) \qquad (1)$$

If equation 1 is assumed to be linear then it can be described
by:

$$PRC_{ss} = mx+b \qquad (2)$$

where

$$m = f \text{ (cycles)}$$

$$x = cycles$$

$$b = f \text{ (temperature)} + f \text{ (DOD)}$$

The slope "m" is determined by the application of a two variable
linear regression method shown in Appendix A to equation 2. The
resulting value of "m" is:

$$m = -\frac{1}{221}$$

Intercept "b" is determined by solving equation 2 for "b".

$$b = PRC_{ss} - mx = PRC_{ss} + \frac{x}{221}$$

TABLE IV

MEASURED STEADY STATE CAPACITY

DOD AND TEMPERATURE CONSTANT FOR 500 CYCLES
AT EACH VALUE

MEASURED CAPACITY	DOD x 100	CYCLES

TEMPERATURE (0°C)

MEASURED CAPACITY	DOD x 100	CYCLES
120	20%	900
111	25%	1200
120	10%	2400
105	40%	3700
99	30%	3800
115	10%	3900
100	20%	4700

TEMPERATURE (10°C)

MEASURED CAPACITY	DOD x 100	CYCLES
120	20%	800
112	25%	1500
115	10%	2400
90	40%	3000

TEMPERATURE (20°C)

MEASURED CAPACITY	DOD x 100	CYCLES
105	20%	900
90	25%	1500
92	10%	2400
82	40%	3000

TEMPERATURE (30°C)

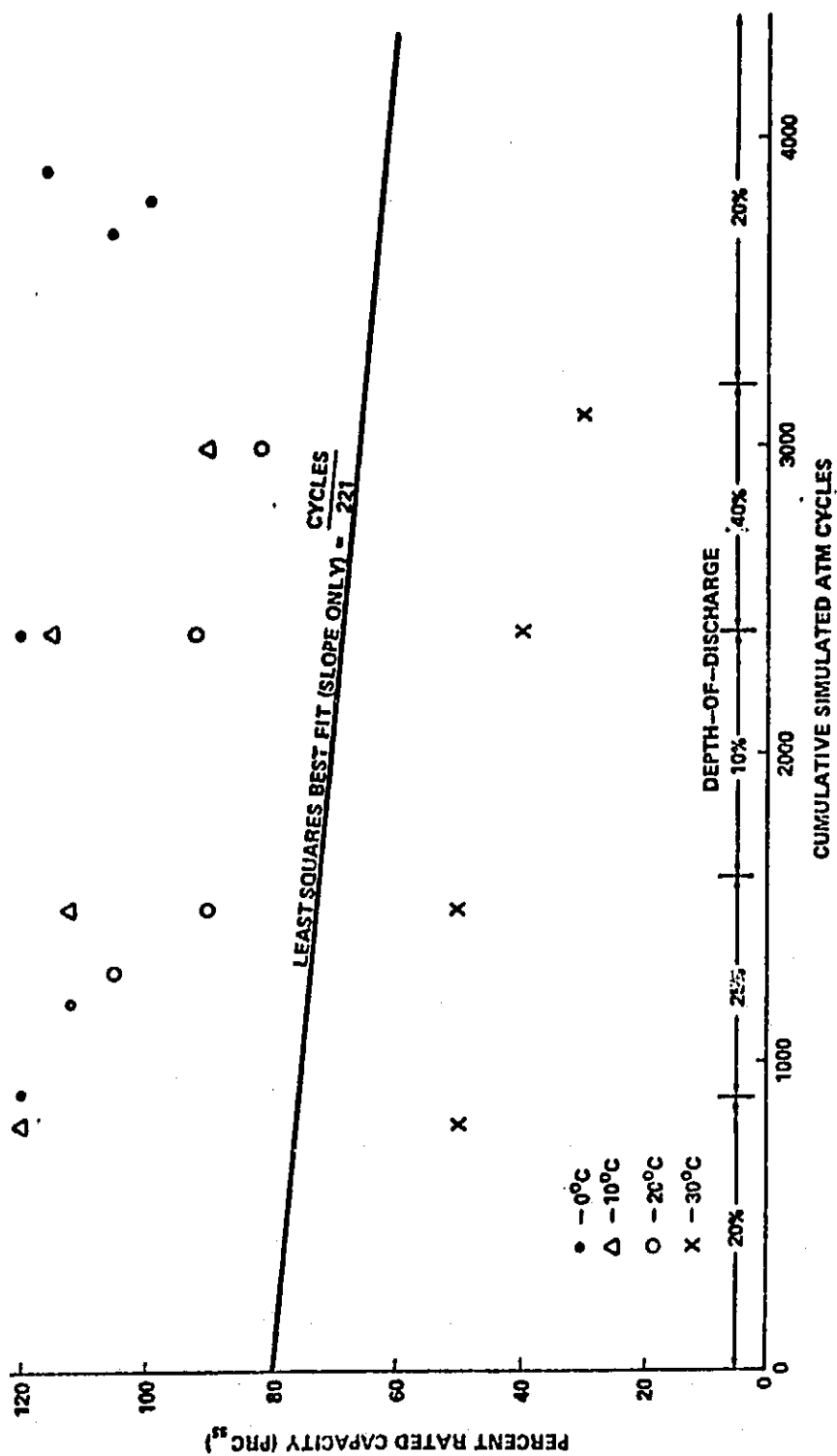| MEASURED CAPACITY	DOD x 100	CYCLES
50	20%	800
50	25%	1500
40	10%	2400
30	40%	3100
35	20%	4700

40M22412

Figure 8. Steady State Capacity Degradation from Table IV
(Each Data Point at Constant T and DOD)

A mean value for "b" at each temperature is shown in Figure 9 where $\bar{b}$ is defined as

$$\bar{b} = \sum \left[\frac{(PRC_{ss(T)}^{-mx}}{N} \right] \quad ; \quad T = 0, 10, 20, 30.$$

The mean values of "b" shown in Figure 9 have an exponential form which can be mathematically described as:

$$\bar{b} = \bar{b}_{0°C} - T^K \tag{3}$$

where

$$T = \text{Degrees Celsius}$$

$$\bar{b}_{0°C} = 125.67$$

By rewriting equation 3

$$T^K = \bar{b}_{0°C} - \bar{b}$$

and taking the logarithm of both sides

$$K_1 \ln T + K_o = \ln \left(\bar{b}_{0°C} - \bar{b} \right)$$

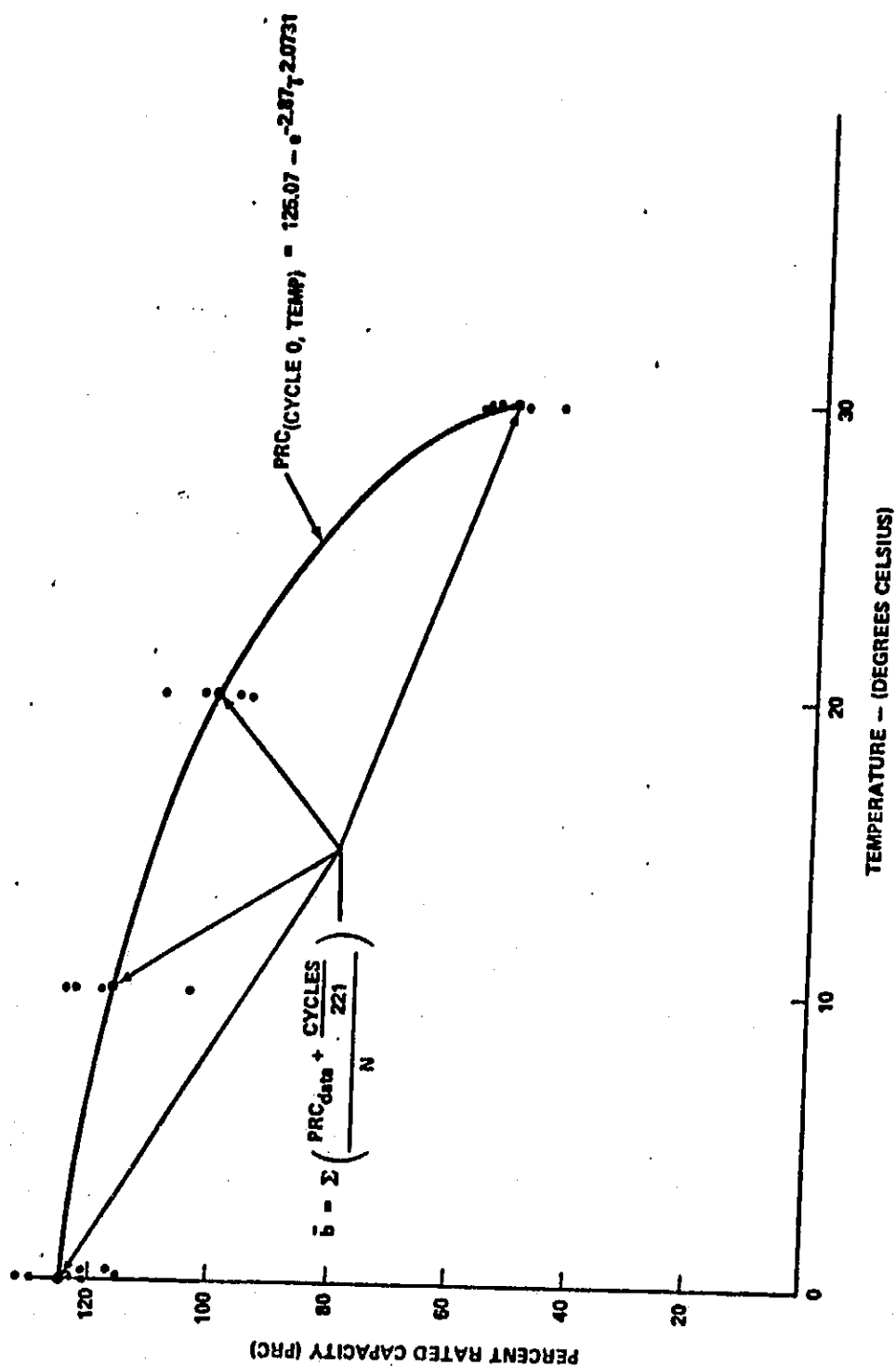A linear equation is acquired. Applying the linear regression methods shown in Appendix A results in

Figure 9. Battery Capacity Temperature
Response Characteristics

$$K_1 = 2.0731$$

$$K_0 = -2.87$$

$$\text{Correlation} = .9919$$

Substituting K_1 and K_0 into equation 3 results in

$$\overset{\cdot}{b} = 125.07 - e^{-2.87} T^{2.0731} \qquad (4)$$

By combining equations 1 and 4 and adding the effects of DOD, the expected capacity can be described as:

$$PRC_{ss} = 125.07 - \frac{x}{221} - e^{-2.87} T^{2.0731} + f(DOD) \quad (5)$$

where

$$x = \text{Cumlative cycles}$$

$$T = \text{Temperature degrees Celsius}$$

$$f(DOD) = \text{effects of DOD}$$

The effects of DOD are calculated by transposing equation 5:

$$PRC_{ss, (Data)} - 125.07 + \frac{x}{221} + e^{-2.87} T^{2.0731} = f(DOD)$$

where

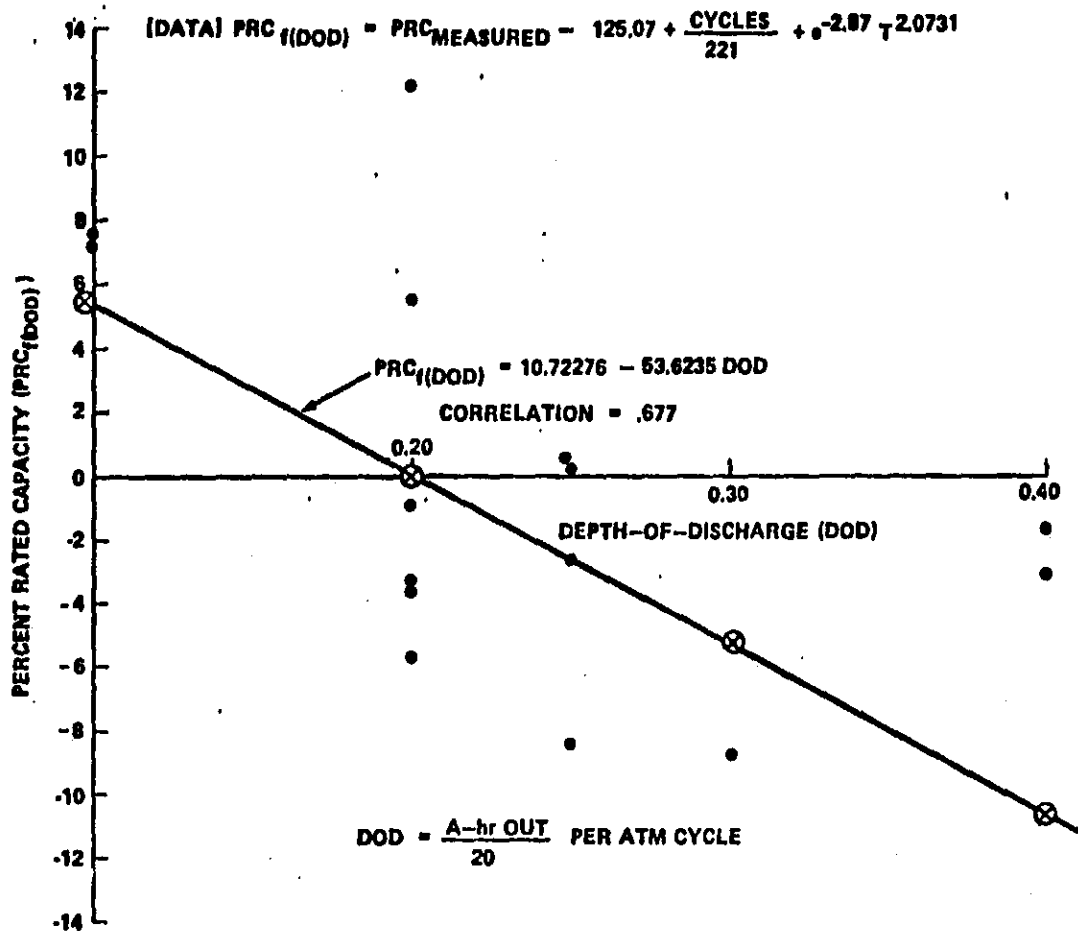$$PRC_{ss (Data)} = \text{Data from Table IV}$$

Figure 10 is a plot of f (DOD) and the respective test DOD at each data point in Table IV. This data can be represented by

$$PRC_{f(DOD)} = K_1 \quad DOD + K_0$$

Application of the linear regression methods in Appendix A

Figure 10. ATM Battery Capacity Response to
Depth-Of-Discharge

The graph shows:

$$[DATA] \; PRC_{f(DOD)} = PRC_{MEASURED} - 125.07 + \frac{CYCLES}{221} + e^{-2.87} T^{2.0731}$$

$$PRC_{f(DOD)} = 10.72276 - 53.6235 \, DOD$$

$$CORRELATION = .677$$

$$DOD = \frac{A-hr \; OUT}{20} \; PER \; ATM \; CYCLE$$

Y-axis: PERCENT RATED CAPACITY ($PRC_{f(DOD)}$)

X-axis: DEPTH-OF-DISCHARGE (DOD)

40M22412

results in:

$$K_1 = -53.6235$$

$$K_0 = 10.72276$$

$$correlation = .627$$

Equation 5 can now be extended by substituting K_1 and K_0.

$$PRC_{ss} = 125.07 - \frac{x}{221} - e^{-2.87} T^{2.0731} + 10.72276$$
$$-53.62 \text{ DOD} \qquad (6)$$

The accuracy of the steady state model, equation 6, is calculated by applying a Chi-squared goodness-of-fit test

$$\chi^2 = \sum \left(\frac{PRC_{data} - PRC_{cal}}{PRC_{cal}} \right)^2$$

where

$$\chi^2_{cal} = 12.4566$$
$$df = 14$$

$$\chi^2_{.95} = 23.7$$
$$\nu = 14$$

Thus there is little difference between the model and the data and the null hypothesis is not rejected. Also,

$$\chi^2_{.05} = 6.57$$
$$\nu = 14$$

indicating that the errors are not small enough to be unbelievable.

40M 22412

The results of the χ^2 test demonstrate that the fit is good but not so good as to make the model unbelievable. The test demonstrates the validity of the basic assumption that the three battery parameters are independent.

Transient Capacity

The ATM battery exhibits two types of transient behavior. The first occurs during the initial 800 cycles of operation when the capacity decays from a nominal 25.4 ampere hours (127 PRC) to the steady state capacity (PRC_{ss}). The second transient condition occurs whenever temperature or DOD changes are imposed on the battery. Determination of the capacity under transient conditions is described with a standard exponential equation.

$$PRC = PRC_{ss} + (Y - PRC_{ss}) \exp\left(\frac{-X_1}{TC}\right) \tag{7}$$

where

PRC_{ss} = Equation 6

Y = PRC_{ss} at beginning of transient condition

X_1 = Cumulative cycles from beginning of transient condition

TC = Time constant

Determination of the time constant (TC) of equation 7 is achieved by first solving equation 7 for the exponential term.

$$\frac{PRC_{data} - PRC_{ss}}{Y - PRC_{ss}} = \exp\left[-\frac{X_1}{TC}\right] \tag{8}$$

Equation 8 can be transformed to linear form by taking the logarithm of both sides.

$$\ln Z = -\frac{X_1}{TC} = K_1 X_1 + K_o \tag{9}$$

where

$$Z = \frac{PRC_{data} - PRC_{ss}}{Y - PRC_{ss}}$$

Since the coefficient of "e" must be one for this model to be applicable, K_o is forced to be zero. Appendix C develops from the normal two variable regression equations the regression equations when K_o equals zero.

A tabulation of the transient data "Z" is contained in Table V. The table however does not contain those values of Z which are zero or negative since these were considered unrealistic and considerably outside the range of expected data. The calculated constants for equation 9 are:

TABLE V

TRANSIENT CAPACITY PERCENTAGE
TIME CONSTANT CALCULATIONS

$$Z = e^{\frac{-X_1}{T_c}} \qquad Z = \frac{Data - PRC_{ss}}{\cdot Y - PRC_{ss}}$$

BATT 1

Z	CYCLES
1.0	0
.87	20
.83	270
.32	950
1.0	0
.45	400
1.0	0
.333	450
.5	550

BATT 3

Z	
1.0	0
.1066	400
.053	600
.026	700
1.0	0
.418	200
.116	400
1.0	0
.83	150
.666	300
1.0	0
.3846	200
.0369	400
.2307	600

BATT 2

Z	CYCLES
1.0	0
.44	150
.333	300
.555	600
1.0	0
.5312	100
.3125	300
.0625	500
.0312	800
1.0	0
.34	200
1.0	0
.05	200
.0125	300
1.0	0
.29	200
.0595	300

BATT 4

Z	CYCLES
1.0	0
.926	20
.67	100
.48	250
.3529	400
.35	500
1.0	0
.1066	100
.1333	200
.04	250
1.0	0
.127	200
.14	400
.12	600
1.0	0
.45	150
.13	250
1.0	0
.48	200
.35	300
.11	750

40M22412

$$K_1 = - \frac{1}{222.25}$$

$$K_o = 0$$

Correlation = .94096

The standard error of estimate is:

$$S^2_{y.x} = .15059$$

and

$$S_{y.x} = \sqrt{.15059} = .38806$$

A plot of the regression equation and the 3 $S_{y.x}$ limits are contained in Figure 11. Rejection of the negative data is justified by the 3 $S_{y.x}$ limits.

Equation 7 can now be completed.

$$PRC = PRC_{ss} + (Y - PRC_{ss}) e^{-\frac{X_1}{222.75}} \tag{10}$$

where

$$PRC_{ss} = 135.07 - \frac{X}{221} - e^{-2.87} T^{2.0731}$$

$$-53.62 \; DOD$$

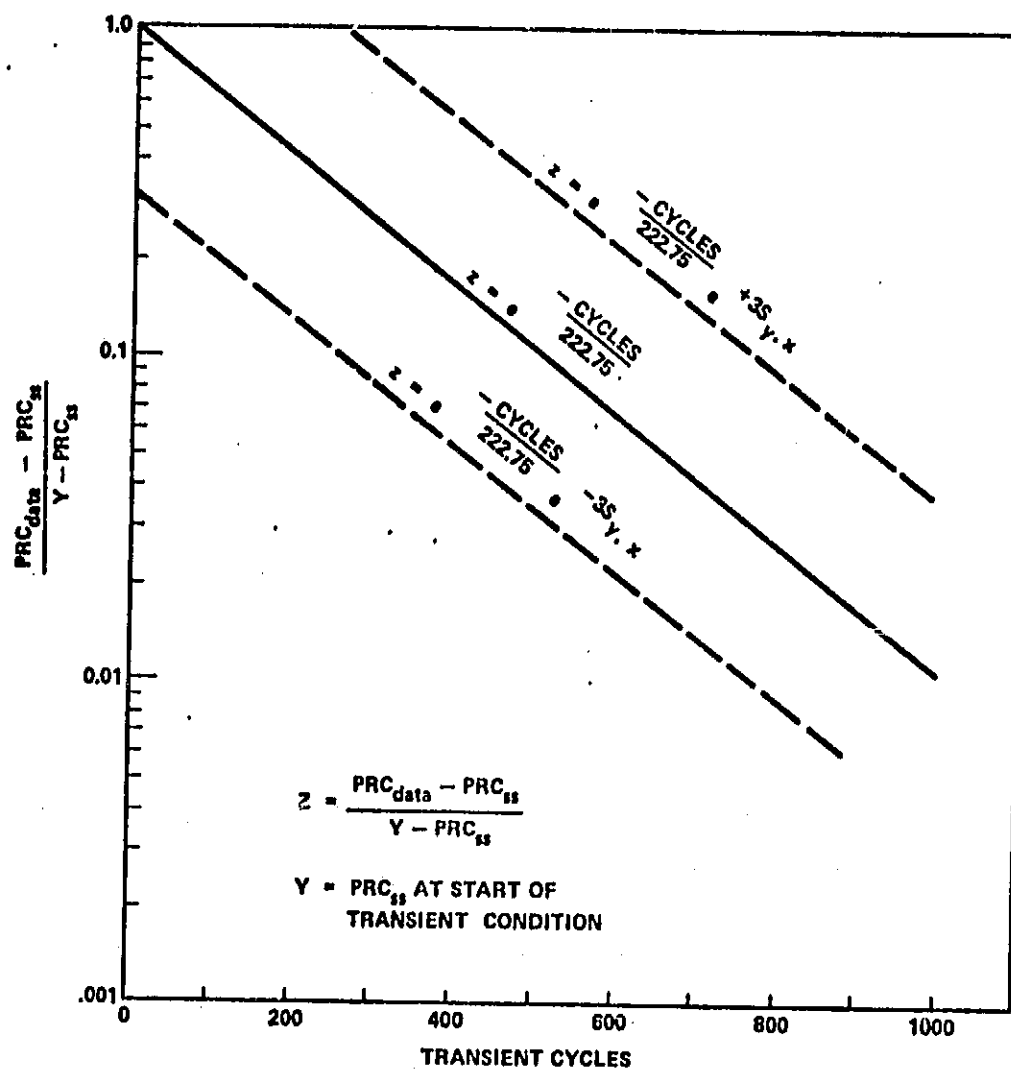Y = PRC_{ss} at beginning of transient

    condition

X_1 = Cycles from beginning

    of transient condition

X = Cycles from beginning of life

T = Degrees Celsius

DOD = $\frac{\text{A-hr out on discharge}}{20 \text{ A-hr}}$

$$Z = \frac{PRC_{data} - PRC_{ss}}{Y - PRC_{ss}}$$

$Y = PRC_{ss}$ AT START OF TRANSIENT CONDITION

TRANSIENT CYCLES

Figure 11. Transient Capacity Characteristics
GE-AB12 20 A-hr Ni-Cd Battery

40M 22412

A plot of the initial transient condition and the steady state
capacity at 20 percent DOD is shown in Figure 5 and 12. A com-
plete model of all the test conditions and the original data is
shown in Figures 13 and 14.

Model accuracy appears to be questionable in two areas. One
of these occurs at cycle 400 battery B2 and cycle 2500 battery
B1 shown in Figure 13. The indicated differences between the
actual and the model capacity is judged to be the effect of cell
failure which the model is not designed to reflect. The cell
failures experienced on batteries B1 and B2 were partial internal
cell short circuits which progressively worsened. Cell charge
retention tests performed on the low cells of batteries B1 and B2
indicate internal cell short circuits. Upon removal of the low
cells, the measured capacity of the remaining cells were again
reflected by the model. The capacity model as presently
constituted does not incorporate cell life considerations. It
was speculated that the short circuits were caused by excessive
physical pressure. The ATM flight cells were modified to relieve
the pressure experienced in the test cells.

It is important to note that the developed models reflect data
acquired from specific cells. The models therefore do not necessar-
ily reflect all makes and models of cells. On cells which contain
more electrolyte per cell area, steady state degradation is affected
more by DOD than by temperature. Model modifications, however, are
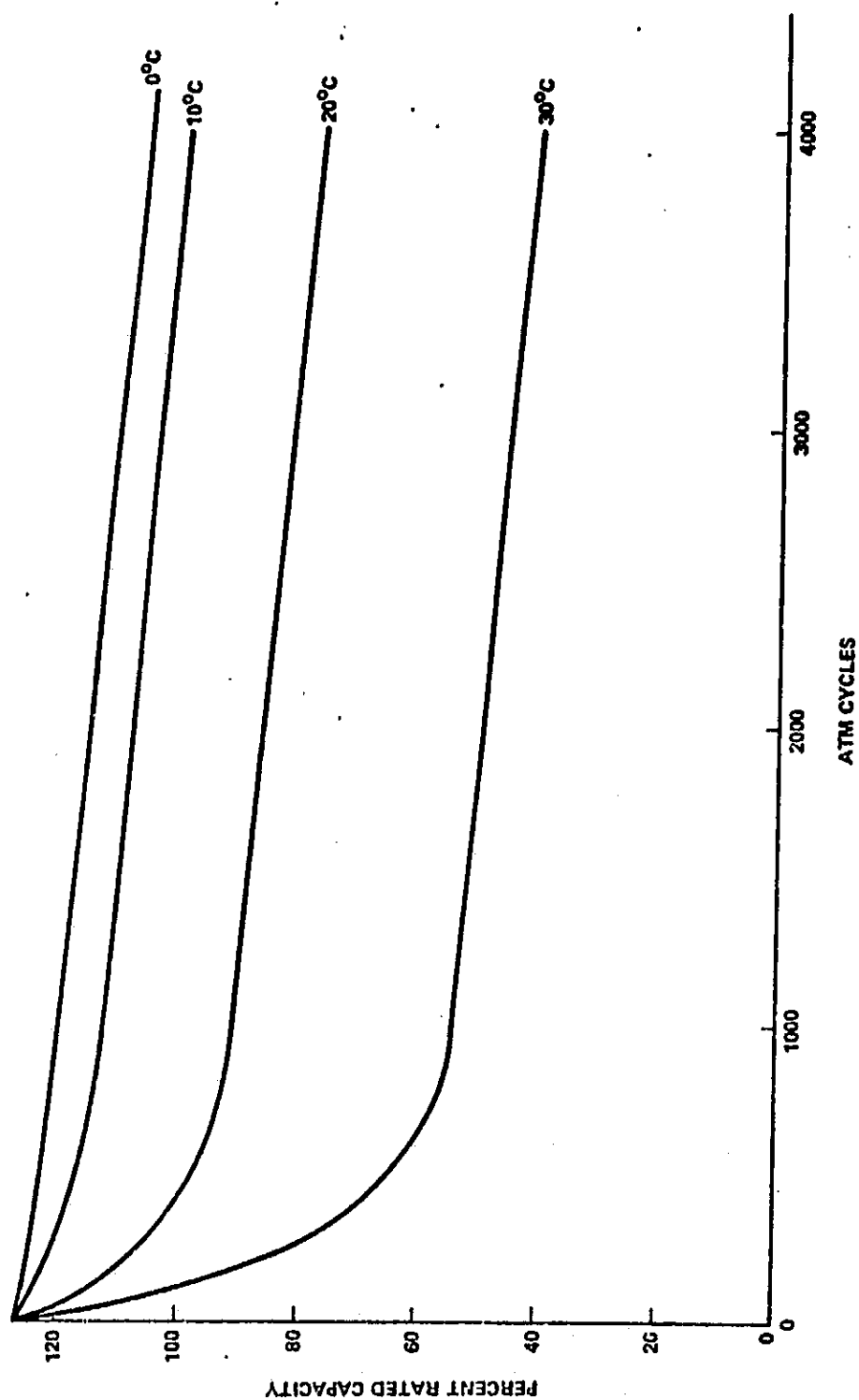easily accomplished because of the parameter independence. The equations

40M224/2

Figure 12. Expected Capacity Degradation
Temperature and DOD Constant
(20% DOD)
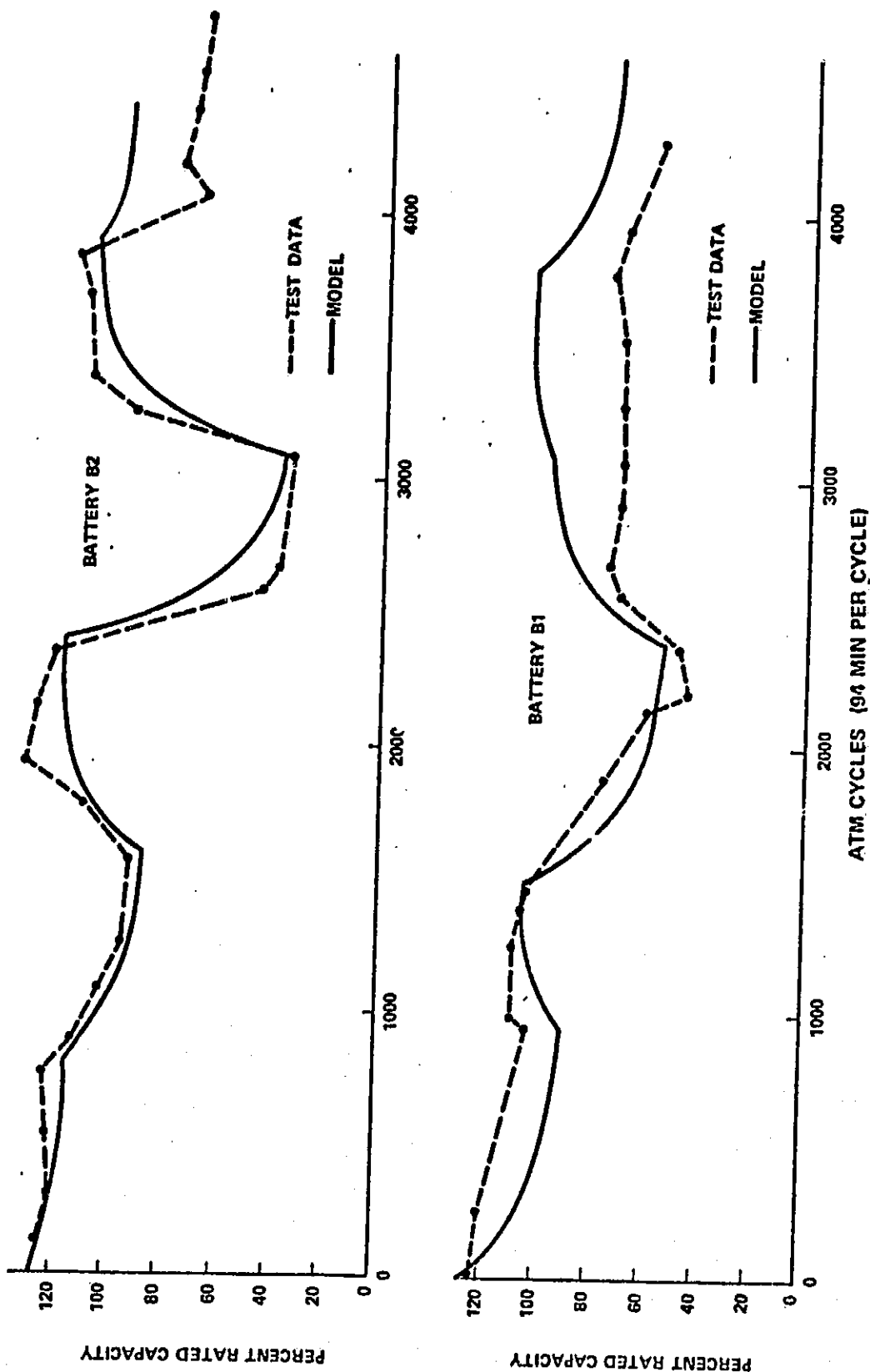
40M22412

Figure 13. Expected and Actual Capacity Degration ATM 20 A-Hr Battery

Figure 14. Expected and Actual Capacity Degradation
ATM 20 A-Hr Battery

can be modified to reflect variations in temperature or DOD caused by cell design, vendor, or other measured changes. The other parameters, initial capacity and degradation rate, can also be easily modified.

Charge Acceptance

Knowledge of Ni-Cd cell charge acceptance efficiency is important in a practical sense when charging is performed on a noncontinuous basis such as would occur during the earth resources portion of the Skylab mission. On a more fundamental basis, knowledge of the charge acceptance efficiency also explains the variation of the charging requirements as a function of charge rate, temperature, and depth-of-discharge.

The charge acceptance data shown in Figures 6 and 7 is average data, that is each point on the curve represents the average charge acceptance efficiency to that state-of-charge (SOC).

If the available battery charge is defined as:

$$Charge_{out} = Charge_{in} - Charge_{loss}$$

Then

$$\frac{Charge_{out}}{Charge_{in}} = 1 - \frac{Charge_{loss}}{Charge_{in}}$$

where

$$\frac{Charge_{out}}{Charge_{in}} \times 100 = C_a = \% \text{ Average Charge Acceptance Efficiency}$$

$$\frac{Charge_{loss}}{Charge_{in}} \times 100 = C_L = \% \text{ Loss Factor} = f(SOC, Temp, Charge Rate).$$

The loss factor can be further subdivided as:

$$\% \text{ Loss Factor} = C_{L_{(SOC=0)}} + C_{L_{[f(SOC)]}}$$

Assuming the charge efficiency at zero SOC is equivalent to that at five percent SOC as shown in Figures 6 and 7, the charge efficiency (Ca) at zero SOC can be defined as:

$$C_a = 100 - C_{L_{(SOC=0)}}$$

Since Bauer[2] describes charge acceptance as proportional to charge rate and inversely proportional to temperature, a model which describes these parameters in terms of losses is of the form:

$$C_{L_{(SOC=0)}} = \frac{T^{K_1}}{R^{K_2}} = 100 - Ca \qquad (11)$$

where

    T = Temperature $^{\circ}C$

    R = Charge Rate in Amperes

Taking the logarithm of both sides of equation 11:

$$\ln C_{L_{(SOC=0)}} = K_1 \ln T + K_2 \ln R + K_0 \qquad (12)$$

Equation 12 is linear with three unknowns. Using the linear regression equations shown in Appendix B, the calculated unknowns are:

    K_0 = -1.19814

    K_1 = 1.09436

    K_2 = -1.1063

Correlation = .96

40M 22412

The charge efficiency model at SOC = 0 can be defined as:

$$C_a(SOC) = 100 - (0.331) \frac{T^{1.094}}{R^{1.1063}} - f(SOC) \qquad (13)$$

Rewriting equation 13:

$$f(SOC) = 100 - (0.331) \frac{T^{1.094}}{R^{1.1063}} - C_a = C_L(f(SOC))$$

and since f(SOC), from Figures 6 and 7, has an exponential form, it can be described by:

$$f(SOC) = \left(\frac{SOC}{10}\right)^K = C_L(f(SOC))$$

SOC is reduced by a factor of $\frac{1}{10}$ to keep the equation constants within reason . By taking the logarithm of both sides:

$$\ln f(SOC) = K_1 \ln \frac{SOC}{10} + K_0 \qquad (14)$$

Values of K_0 and K_1 were determined by using the data in Table III and the linear regression methods shown in Appendix A. The calculations were based on all positive values of f(SOC) in equation 14. Rejection of negative values of f(SOC) was justified by the 3 $S_{y.x}$ limits shown in Figure 15. The calculated values are:

$K_0 = -13.2787$

$K_1 = 6.0567$

Correlation = 0.9286

$S_{y.x} = .3555$

The complete charge efficiency equation is now defined as:

$$C_a = 100 - (0.331) \frac{T^{1.094}}{R^{1.1063}} - 1.71 \times 10^{-6} \left(\frac{SOC}{10}\right)^{6.0567} \quad (15)$$

4042224412

$$f(soc) = 100 - 0.331 \frac{T^{1.09814}}{R^{1.1063}} - TEST\ DATA$$

$$f(soc) = e^{-K_o}\left(\frac{soc}{10}\right)^{K_1}$$

$$f(soc) = e^{-13.2787}\left(\frac{soc}{10}\right)^{6.0567}$$

$3\ S_{y \cdot x}$
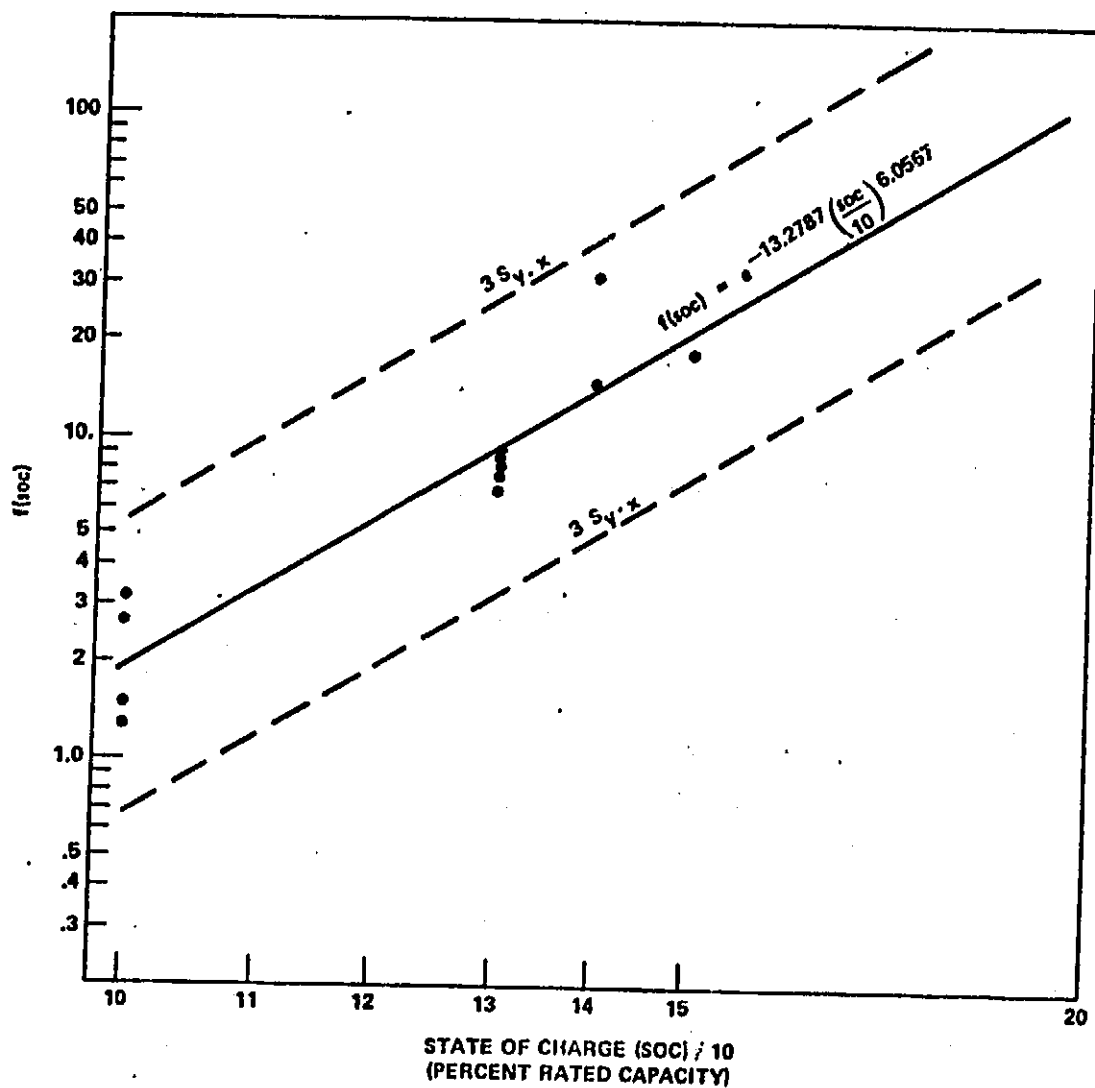
$3\ S_{y \cdot x}$

f(soc)

STATE OF CHARGE (SOC) / 10
(PERCENT RATED CAPACITY)

Figure 15.   Ni-Cd Cell Charge Acceptance As A
Function of SOC
ATM - 20 A-hr Cell

40M22412

A check on the accuracy of equation 15 is conducted by using a Chi-squared goodness of fit test.

$$\chi^2_{cal} = \sum \left(\frac{C_{a,data} - C_{a,model}}{C_{a,model}} \right)^2$$

$$\chi^2_{cal} = 25.0863 \qquad \text{and} \qquad \chi^2_{.95} = 25$$
$$df\ 15 \qquad\qquad\qquad\qquad\qquad\qquad \upsilon = 15$$

Although it appears from the above calculations that the null hypothesis should be rejected, the exclusion of one outlier, which was also excluded in the model development, considerably improved the accuracy of the model. The outlier is the result of the testing difficulties mentioned in chapter one. Recalculation of the Chi squared test:

$$\chi^2_{cal} = 6.966$$
$$df = 14$$

$$\chi^2_{.95} = 23.7$$
$$df = 14$$

These results show that the null hypothesis is not to be rejected. In fact:

$$\chi^2_{.05} = 6.57$$
$$df = 14$$

indicating exceptional model accuracy.

Although the average charge efficiency (C_a) was the measured value, the instantaneous charge efficiency is of greater importance. The instantaneous charge efficiency C_N is derived in the following manner from Figure 12.

$$C_a SOC = C_1 \Delta SOC + C_2 \Delta SOC + \cdots + C_N \Delta SOC$$

where

$$C_1, \cdots, C_N = \text{average charge efficiency within the SOC}$$
interval. In the limit as SOC approaches zero, C_N = instantaneous charge efficiency.

Solving for C_N

$$C_N = \frac{C_a SOC - [C_1 \Delta SOC + C_2 \Delta SOC + \cdots, C_{N-1} \Delta SOC]}{\Delta SOC}$$

but

$$C_1 \Delta SOC + C_2 \Delta SOC + \cdots + C_{N-1} \Delta SOC = C_{a_{N-1}} (SOC - \Delta SOC)$$

therefore

$$C_N = \frac{C_a SOC - C_{a_{N-1}} (SOC - \Delta SOC)}{\Delta SOC}$$

If we write

$$K_3 = \frac{SOC}{\Delta SOC}$$

then

$$C_N = C_a K_3 - C_{a_{N-1}} (K_3 - 1) \qquad (16)$$

where

C_N = Average charge efficiency within ΔSOC interval

$$K_3 = \frac{SOC}{\Delta SOC}$$

Equation 16 can be simplified by substituting the following two forms of equation 15:

$$C_a = K_1 - K_4 \left(\frac{SOC}{10}\right)^{K_2}$$

$$C_{a_{N-1}} = K_1 - K_4 \left(\frac{SOC - \Delta SOC}{10}\right)^{K_2}$$

where from equation 15

$$K_1 = 100 - \frac{T^{1.09814}}{R^{1.1063}} \ (0.331)$$

$$K_2 = 6.0567$$

$$K_4 = 1.71 \ \times \ 10^{-6}$$

substituting

$$C_N = \left[K_1 - K_4 \left(\frac{SOC}{10}\right)^{K_2}\right] K_3 - \left[K_1 - K_4 \left(\frac{SOC - \Delta SOC}{10}\right)^{K_2}\right] [K_3 - 1]$$

(17)

and simplifying

$$C_N = K_4 \left(\frac{\Delta SOC}{10}\right)^{K_2} \left[(K_3 - 1)^{K_2 + 1} - (K_3)^{K_2 + 1}\right] + K_1 \qquad (18)$$

When all appropiate values are substituted equation 18 becomes:

$$C_N = \frac{1.5 \times 10^{-12}}{\Delta SOC} \left[(SOC - \Delta SOC)^{7.0567} - SOC^{7.0567}\right] + K_1$$

(19)

where

SOC = percent state-of-charge.

Plots of the average and instantaneous charge efficiency models (C_a, equation 15, and C_N, equation 19) are shown in Figures 16 through 19.
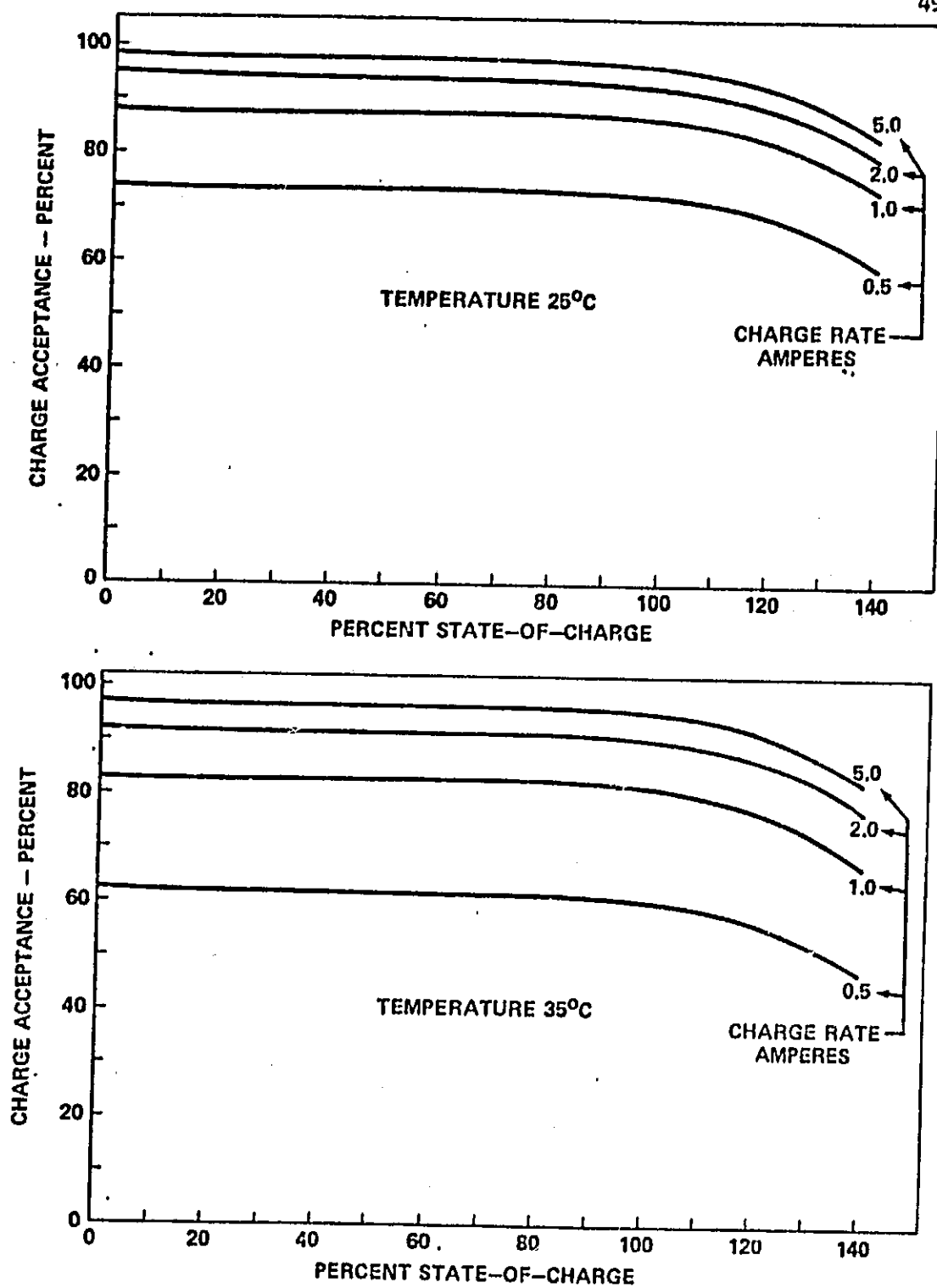
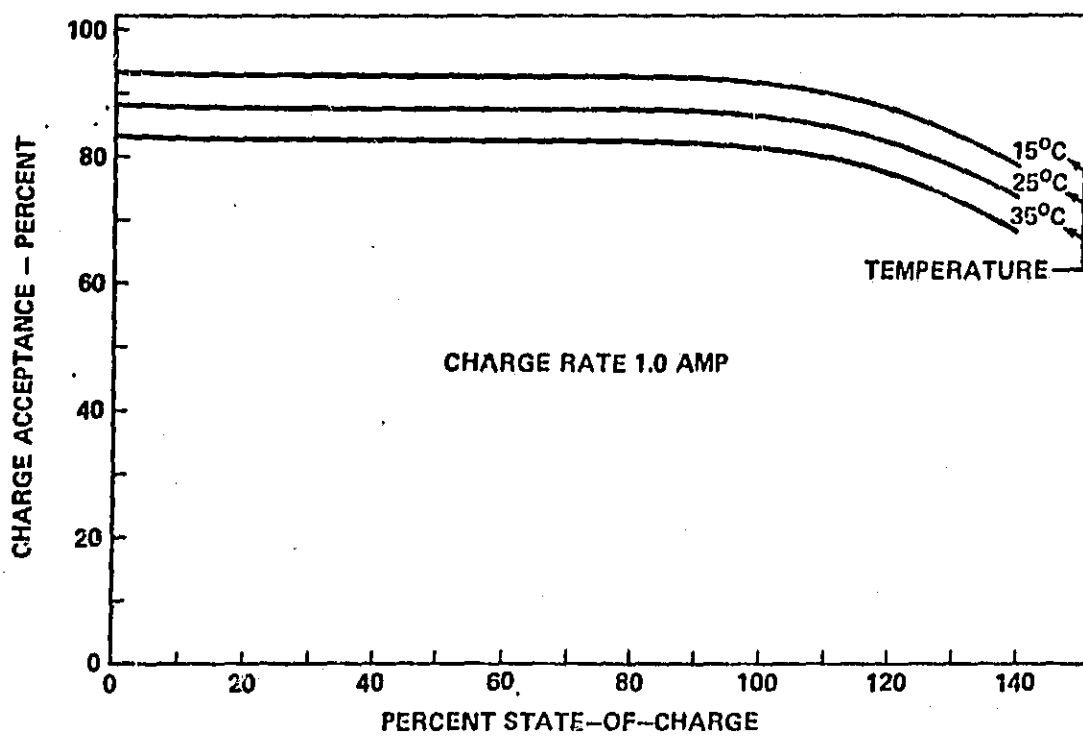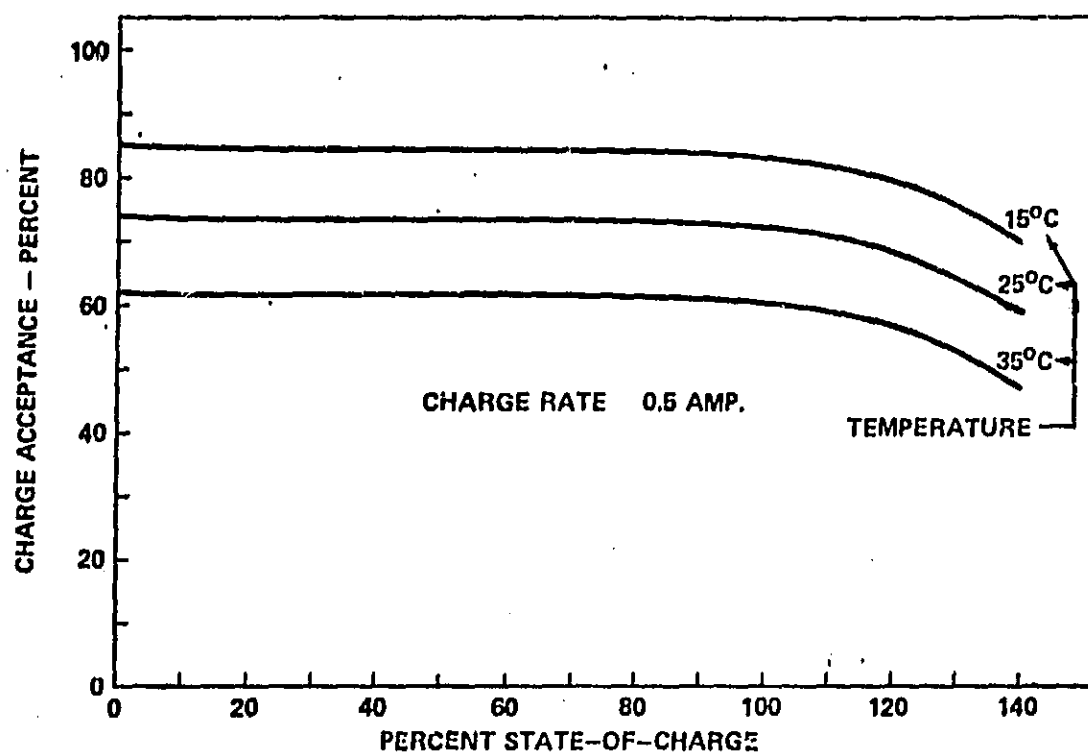Figure 16. Average Charge Acceptance
AB12-G Ni-Cd Cell

4042412

Figure 17. Average Charge Acceptance
AB12-G Ni-Cd Cell
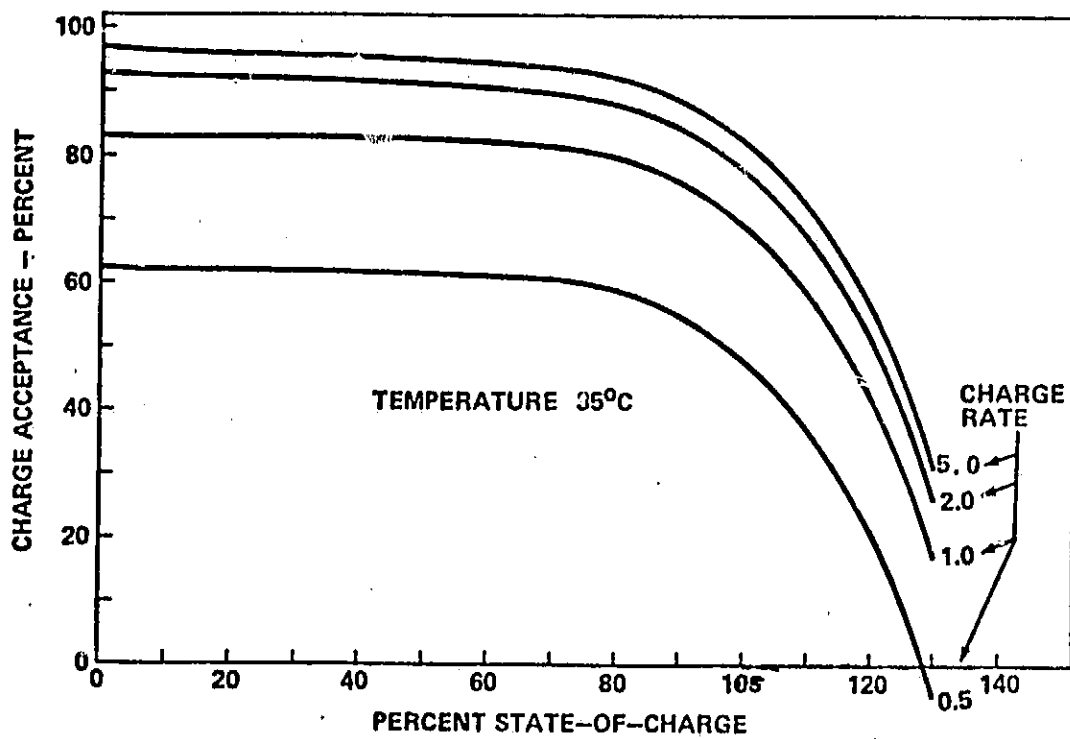
40M 22412
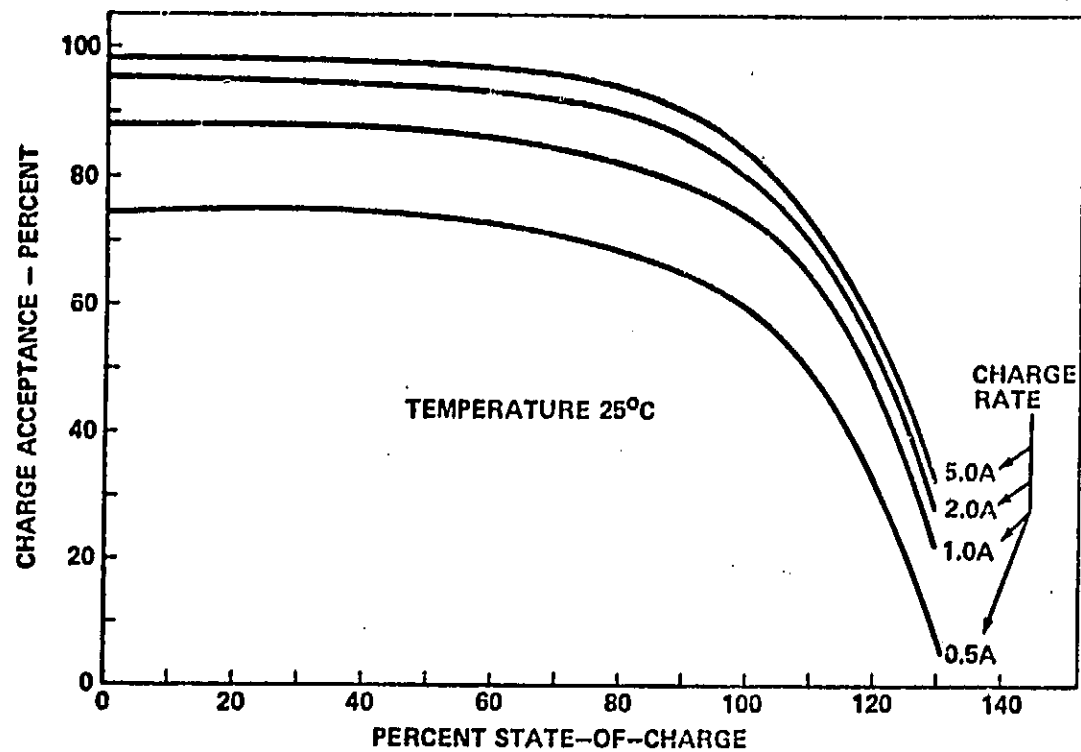
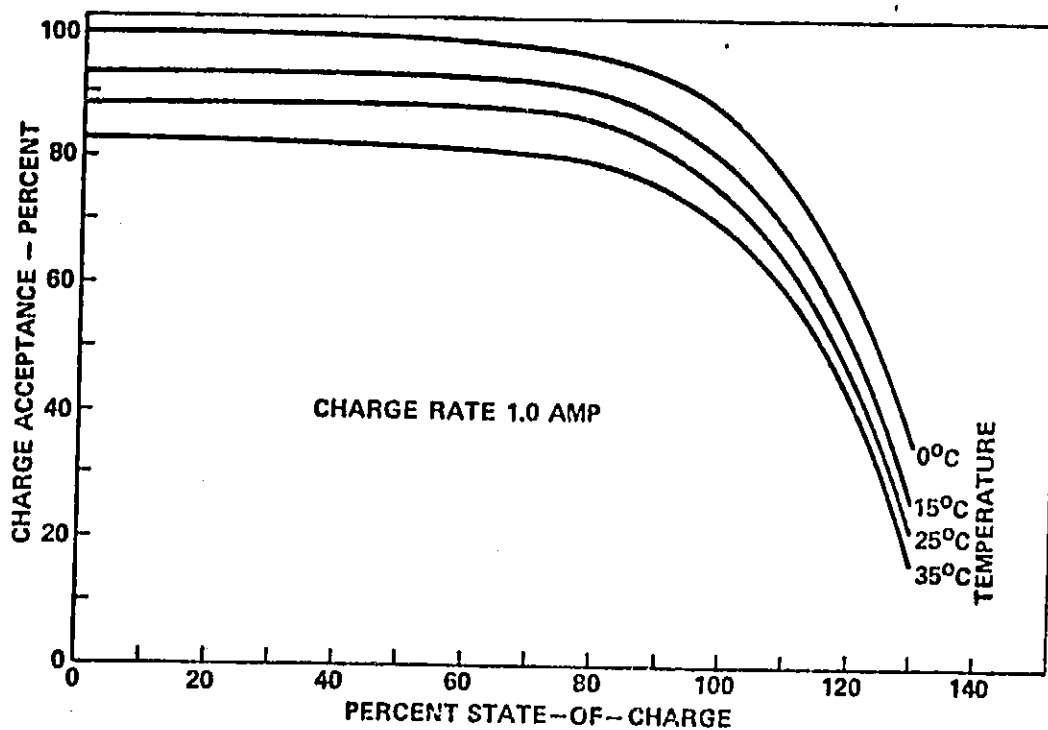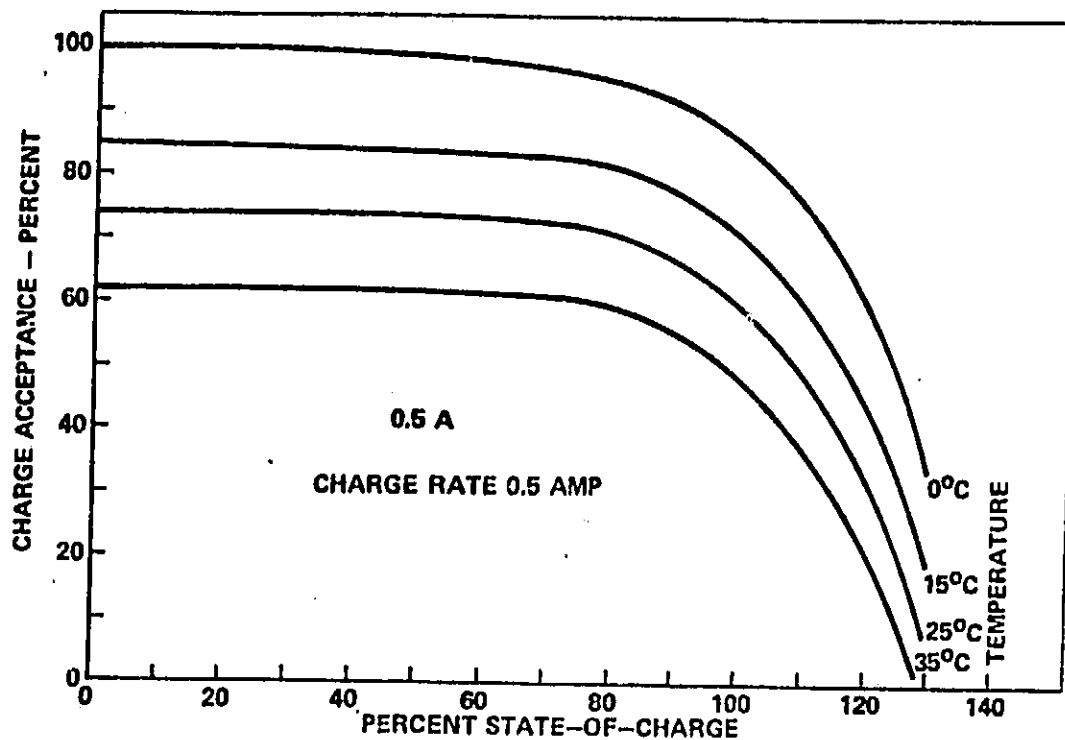Figure 18. Instantaneous Charge Acceptance
AB12-6 Ni-Cd Cell

40M22412

Figure 19. Instantaneous Charge Acceptance
AB12-G Ni-Cd Cell

40M22412

PERFORMANCE PREDICTION MODEL SUMMARY

Performance prediction model development was based on experimental data from 20-ampere-hour GE AB12 type cells. Although the models were directed to a specific application, namely the Skylab ATM mission, the results of the experimental data and the model forms lend themselves readily to general Ni-Cd battery application. Three basic performance models have been developed: capacity degradation, average charge acceptance, and instantaneous charge acceptance.

The capacity degradation model describes the expected usable battery capacity as a function of cyclic time, temperature, and depth-of-discharge. The transient effects as a result of parametric variations are also described. Although beyond the scope of this program, a complete factorial experimental program to verify the assumptions of parameter independence would be desirable.

It is important to note that the model does not reflect the life or cell failure characteristics of Ni-Cd cells. A probabilistic model would be more applicable to describe the expected cell life, and specific test data should be acquired for this type of model.

The average charge acceptance model is described as a function of charge rate and temperature and is based on experimental data. The instantaneous charge acceptance model is derived in terms of the average charge acceptance model. When these models are used

to describe other cell types, the absolute capacity of the cell must be ascertained. The absolute capacity of the ATM cell is 140 percent of rated capacity. Other cell types may be different and in that case the model constants must be modified.

Although all the models describe a range of cell and battery performance within the optimum Ni-Cd battery operating range, data and battery response beyond the present range would be desirable. Extending the data ranges would provide operating limits on cell performance in terms of performance degradation, physical degradation, and environmental failure limits. Other desirable cell operating characteristics, previously mentioned, are the cell and battery ageing characteristics as a function of time and various operating parameters, failure modes, and probabilities.

The ultimate in battery models would be those that reflect the effects of plate design and loading, electrolyte loading, precharge, and internal gas control. This type of model would be very useful in the capacity degradation model where the degradation rate has been observed to be very sensitive to electrolyte loading. Until the ultimate model is developed however, the three models described provide some measure of cell and battery operating information, control, and performance prediction.

4011.2.2 412

APPENDIX A
LINEAR REGRESSION WITH TWO UNKNOWNS

The normal equations in two unknowns are:

$$\Sigma X_1 = K_0 N + K_1 X_2$$

$$\Sigma X_1 X_2 = K_0 \Sigma X_2 + K_1 \Sigma X_2^2$$

Solving for K_0 and K_1

$$K_0 = \frac{\Sigma X_1 (\Sigma X_2^2) - \Sigma X_2 (\Sigma X_1 X_2)}{N \Sigma X_2^2 - (\Sigma X_2)^2}$$

$$K_1 = \frac{N \Sigma X_1 X_2 - \Sigma X_1 (\Sigma X_2)}{N \Sigma X_2^2 - (\Sigma X)^2}$$

The corresponding correlation coefficient is

$$CC = \frac{N \Sigma X_1 X_2 - \Sigma X_1 (\Sigma X_2)}{[[N \Sigma X_2^2 - (\Sigma X_2)^2] [N \Sigma X_1^2 - (\Sigma X_1)^2]]^{1/2}}$$

APPENDIX B
LINEAR REGRESSION WITH THREE UNKNOWNS

The normal equations in three unknowns are:

$$\Sigma X = K_0 \ N + K_1 \ \Sigma X_2 + K_2 \ \Sigma X_3$$

$$\Sigma X_1 X_2 = K_0 \Sigma X_2 + K_1 \ \Sigma X_2^2 + K_2 \ \Sigma X_2 X_3$$

$$\Sigma X_1 X_3 = K_0 \Sigma X_3 + K_1 \ \Sigma X_2 X_3 + K_2 \Sigma X_3^2$$

In matrix form the equations reduce to:

$$
\begin{bmatrix} \Sigma X_1 \\ \Sigma X_1 X_2 \\ \Sigma X_1 X_3 \end{bmatrix}
=
\begin{bmatrix} N & \Sigma X_2 & \Sigma X_3 \\ \Sigma X_2 & \Sigma X_2^2 & \Sigma X_2 X_3 \\ \Sigma X_3 & \Sigma X_2 X_3 & \Sigma X_3^2 \end{bmatrix}
\begin{bmatrix} K_0 \\ K_1 \\ K_2 \end{bmatrix}
$$

Cramer's rule or other appropriate solution techniques can be used to solve for K_0, K_1 and K_2.

The appropriate correlation coefficient equations are:

$$CC_{1.2} = \frac{N\Sigma X_1 X_2 - \Sigma X_1 \Sigma X_2}{[[N\Sigma X_1^2 - (\Sigma X_1)^2] \ [N\Sigma X_2^2 - (\Sigma X_2)^2]]^{1/2}}$$

$$CC_{1.3} = \frac{N\Sigma X_1 X_3 - \Sigma X_1 \Sigma_3}{[[N\Sigma X_1^2 - (\Sigma X_1)^2] \ [N\Sigma X_1^2 - (\Sigma X_3)^2]]^{1/2}}$$

$$CC_{2.3} = \frac{N\Sigma X_2 X_3 - \Sigma X_2 \Sigma X_3}{[[N\Sigma X_2{}^2 - (\Sigma X_2)^2] \; [N\Sigma X_3{}^2 - (\Sigma X_3)^2]]^{1/2}}$$

$$CC_{1.2,3} = \frac{(CC_{1.2})^2 + (CC_{1.3})^2 - 2(CC_{1.2})(CC_{1.3})(CC_{2.3})}{1 - (CC_{2.3})^2}^{1/2}$$

LINEAR REGRESSION WITH TWO UNKNOWNS

$$Y = K_1 X + K_0$$

where $K_0 = 0$

The normal equations are

$$\Sigma Y = K_0 N + K_1 \Sigma X$$

$$\Sigma XY = K_0 \Sigma X + K_1 \Sigma X^2$$

which in reduced form yield

$$K_0 = \frac{\Sigma Y \Sigma X^2 - \Sigma X \Sigma X Y}{N \Sigma X^2 - (\Sigma X)^2}$$

$$K_1 = \frac{N \Sigma XY - \Sigma X \Sigma Y}{N \Sigma X^2 - (\Sigma X)^2}$$

$$r = \frac{N \Sigma XY - \Sigma X \Sigma Y}{\left[[N \Sigma X^2 - (\Sigma X)^2][N \Sigma Y^2 - (\Sigma Y)^2] \right]^{1/2}}$$

If $K_0 = 0$

then $\quad K_1 = \dfrac{\Sigma Y}{\Sigma X} \quad$ and $\quad \Sigma XY = \dfrac{\Sigma Y \Sigma X^2}{\Sigma X}$

40M22412

by substitution

$$r = \frac{\dfrac{N \ \Sigma Y \Sigma X^2}{\Sigma X} - \Sigma X \Sigma Y}{[[N\Sigma X^2 - (\Sigma X)^2] \ [N\Sigma Y^2 - (\Sigma Y)^2]]^{1/2}}$$

$$SY.X = \left[\frac{\Sigma Y^2 - K_1 \dfrac{\Sigma Y \Sigma X^2}{\Sigma X}}{N}\right]^{1/2} = \text{standard error of estimate}$$

REFERENCES

(1) Green, Rog G.; <u>Battery Survey Skylab Program Payload Integration</u>.
     Martin Marietta Corporation, December 1970.

(2) Bauer, P.; <u>Batteries for Space Power Systems</u>, Redondo Beach,
     California; 1968 NASA Publication SP-172.

(3) Bauer, P.; Sparks, R. H.; <u>Nickel-Cadmium Batteries for the Orbiting
     Geophysical Observatory</u> . Space Technology Laboratories, Inc.,
     Redondo Beach, California, April 1963.

(4) Horton, W. P.; <u>Performance and Design Requirements Apollo
     Telescope Mount (ATM)</u> General System Specification NASA
     50M02417, Astrionics Laboratory MSFC, February 1969.

(5) Belew, L. F. Haeussermann, W. <u>Apollo Telescope Mount Project
     Development Plan</u>. NASA, MSFC, April 1967.

(6) Sanders, J. A."ATM Cell Testing and Battery Analysis Final
     Report Volume I". Report 40M21617 Marshall Space Flight Center,
     Huntsville, Alabama, March 31, 1971.

(7) Kirsch, W. W.; Shikoh, A. E. "Summary Test Report on Nickel
     Cadmium Batteries for Apollo Telescope Mount", Electrochemical
     Power Section, Astrionics Laboratory, MSFC, NASA, June 1970.

(8) Lombard, J. W.; <u>ATM Power Equipment Operation During Earth
     Resources Experiments and Rendezvous.</u> Sperry Rand Corporation,
     Support Services Division, August 1970.

40M22412

BIBLIOGRAPHY

Carson, W. N., Jr; A Study of Nickel-Cadmium Spacecraft Battery Charge Control. General Electric Company, Research and Development Center; April 1966.

Carson, W. N. Jr.; Rampel, G., Weinstock, I. B.; Characterization of Recombination and Control Electrodes for Spacecraft Nickel-Cadmium Cells. General Electric Company, Battery Business Section; January 1968.

Duncan, A. J.; Quality Control and Industrial Statistics. Richard D. Irwin, Inc., Homewood, Illinois, (1959).

Gladstone, B.; Yuh, J.; Optimum Charging System Study Program. Gulton Industries, Engineered Magnetics Division, August 1966.

Hicks, C. R.; Fundamental Concepts in The Design of Experiments. Holt, Rinehart, and Winston, New York, (1964).

Hinkle, H. W.; Smith, O. D.; Skylab Program Payload Integration, Electrical Power System Analyses. Martin Marietta Corporation, Aerospace Group, December 1970.

Lerner, S.; Seiger H. N.; Characterization of Recombination and Control Electrodes for Spacecraft Nickel-Cadmium Cells. Gulton Industries, Alkiline Battery Division, September 1966.

40M 2.2 4/12

Spiegel, M. R.; STATISTICS. Schaum's Outline Series

Voygentizie, P. R.; Rampel, G. G.; Carson, W. N. Jr. Characterization of Recombination and Control Electrodes for Spacecraft Nickel-Cadmium Cells. General Electric Company, Battery Business Section, March 1970.